

Nanofluids for Heat Transfer Enhancement-A Review

E.K. Goharshadi*, H. Ahmadzadeh, S. Samiee and M. Hadadian

Department of Chemistry, Ferdowsi University of Mashhad, Mashhad 91779, Iran

(Received 12 December 2012, Accepted 28 March 2013)

A nanofluid is a dilute liquid suspension of particles with at least one critical dimension smaller than ~ 100 nm. Researches so far suggest that nanofluids offer excellent heat transfer enhancement over conventional base fluids. The enhancement depends on several factors such as particle shape, particle size distribution, volume fraction of nanoparticles, temperature, pH, and thermal conductivities of nanoparticles and base fluids.

This paper presents an updated review on nanofluids with the emphasis on heat transfer enhancement including formulation, physical properties, biological and non-biological applications, stability, possible mechanisms for the enhancement of heat conduction, and numerical modelling of nanofluids. Based on the research findings, a number of challenges are emphasized in order to understand the underlying physics for future industrial take-up of the nanofluids technology. Further computational studies are also required in order to understand all of the factors affecting on the enhancement of thermal conductivity of nanofluids.

Keywords: Heat transfer enhancement, Nanofluids, Thermal conductivity, Viscosity

INTRODUCTION

Scientists have been quite active in the past few decades in the search of novel approaches to increase heat dissipation of various cooling devices. These include many electronics devices such as microprocessors where continually increasing power densities require more innovative techniques of heat dissipation. Heat transfer through a fluid medium is important in several engineering applications including heat exchangers, refrigerators, automobiles, and power plants. The ability of a fluid medium to transfer heat across a small temperature difference enhances the efficiency of energy conversion and improves the design and performance of automobile engines, heat transfer devices, and micro-electro-mechanical systems (MEMS).

In recent years, modern technologies have permitted the manufacturing of a new class of fluids, called nanofluids. A nanofluid is the promising heat and mass transfer medium in which nanoparticles are dispersed. It is known that the thermal conductivity of the nanofluids is considerably higher than that

of the corresponding base fluids [1,2]. The enhancement depends on several factors such as particle shape, particle size, volume fraction of particles, and thermal properties of solid and liquid.

In spite of the potential and features of nanofluids, these rather special fluids are still in their early development stages. The experimental data on physical properties of nanofluids especially thermal conductivity are very scattered. Even though data provide insight into nanofluid properties and heat transfer benefits, a considerable amount of research remains to be done on this subject and the development of the field faces several challenges.

The present review provides a comprehensive outline of the attractive research progress made in the area of nanofluids. It also summarizes the experimental, theoretical, and computational developments of the field.

PRE-NANOFLUID STUDIES OF HEAT TRANSFER FLUIDS

Heat transfer fluids such as water, mineral oil, and ethylene glycol play a vital role in many industrial processes

*Corresponding author. E-mail: gohari@ferdowsi.um.ac.ir

including power generation, chemical processes, heating or cooling processes, and microelectronics.

Heat transfer technology stands at cross roads today between ever increasing demand of cooling ultra-high heat flux equipments on one hand and unprecedented pace of miniaturization on the other. In the present days, the different ranges of laser applications, superconducting magnets, high power X-ray, and above all super-fast computing chips performing trillions of operations per second are becoming quite common. These devices are not only to operate in their respective applications with high precision but also to do so occupying minimum space [3].

Today's rapid IT development requires PC performance capable of fast data processing. To meet this requirement, high-performance devices built in PCs have been developed. Especially, competitive release of faster CPU products and shift towards more compact and thinner devices is noticeable. This leads to higher heat generation because of CPU temperature rise and causes the short life, malfunction, and failure of CPUs. CPU cooling has been taken seriously. Pentium-IV CPU and Athlon XP, released by Intel and AMD respectively, has high heat dissipation, requiring excellent cooling performance. For example, 2 GHz Pentium-IV processor made in 0.18 μm manufacturing process has thermal design power (TDP) of 75.8 W, requiring cooling performance of 0.47 $^{\circ}\text{C}/\text{W}$ (at 40 $^{\circ}\text{C}$). 2 GHz Pentium-IV processor made in 0.13 μm manufacturing process has a little lower TDP 52 W and requires cooling performance of 0.53 $^{\circ}\text{C}/\text{W}$ (at 40 $^{\circ}\text{C}$) [4]. This puts a challenge not only to the core device design but also to their thermal management. While air based cooling systems are more common and reliable, they fail miserably with increasing heat flux. Therefore, in almost all of the high heat flux applications liquid cooling is preferred. The cooling liquids usually used are water/chilled water, common refrigerants, and liquid nitrogen, or similar cryogens depending on the specific application. Usual refrigerants are hazardous to the environment and cryogens are costly not only due to their energy intensive production process but also due to whole range of costly equipments which use them. While water is a convenient and safe medium, its relatively poor heat transfer characteristic is a major disadvantage [3].

Solid particles generally possess far greater thermal conductivity than conventional heat transfer fluids as seen in

Table 1. The thermal conductivity of copper, for example, is 700 times higher than that of water and 3000 times that of engine oil. Mixing solid particles in a liquid can, therefore, enhance the cooling potential of the liquid by increasing the thermal conductivity of the suspended fluid. Working on various mixtures using millimetre or micrometer size particles gets back to over a hundred years ago [5-7].

While these fluids do provide the aforementioned cooling benefits, their implementation is complicated by their causing severe problems. In practical applications, the abrasive action of the particles causes the clogging of flow channels, erosion of pipelines, and their momentum lead to an increase in pressure drop in practical applications. Furthermore, they often suffer from instability and rheological problems. In particular, the particles tend to settle rapidly. Thus, although these fluids give better thermal conductivities, their use is not practical.

Recently, the advent and development of nanotechnology offers the opportunity to enhance the application of heat transfer fluids by introducing nanofluids. A nanofluid is a class of solid-liquid composite materials consisting of solid nanoparticles dispersed in a heat transfer fluid. The concept of nanofluids was first materialized by Choi [1] after performing a series of research at Argonne National Laboratory in USA. The first experiments were done by Masuda *et al.* [8] to show the extraordinary values of thermal conductivity of nanofluids. However, subsequent research [2,9,10] showed that the nanofluids exhibit higher thermal conductivity even for low concentration of suspended nanoparticles. For instance, experiments showed an increase in thermal conductivity by dispersion of less than 1% volume fraction of Cu nanoparticles or carbon nanotubes (CNTs) in ethylene glycol or oil by 40% and 150%, respectively [11].

POTENTIAL AND FEATURES OF NANOFUIDS

The following features for different nanofluids have been observed consistently by different researchers at various organizations:

1. The most important feature observed in nanofluids is an abnormal rise in thermal conductivity, far beyond expectations, and much higher than any theoretical prediction. Comparing to pure liquids, the thermal conductivity of

Table 1. Thermal Conductivity Values and Measuring Temperature of Thermal Conductivity for Some Solids and Liquids

Material	Thermal conductivity (W m ⁻¹ K ⁻¹)	Measuring temperature (K)
Metallic solids		
Aluminium (Al)	237	293
Copper (Cu)	401	273-373
Gold (Au)	318	273-373
Iron (Fe)	80.40	273-373
Silver (Ag)	429	300
Non-metallic solids		
Alumina (Al ₂ O ₃)	40	
CNT	3000	
Copper oxide (CuO)	76.50	
Diamond	3300	
Fullerene	0.40	
Silicon (Si)	148	
Liquids		
Ethylene glycol	0.20	
Engine oil	0.14	
Glycerol	0.29	293
Water	0.61	293

nanofluids depends strongly on to temperature increase. The large surface area of nanoparticles allows for more heat transfer.

2. Abnormal viscosity increase relative to the base fluid.
3. Stability. Because the nanoparticles are small, they weigh less, and the sedimentation rates are smaller. Nanofluids have been reported to be stable over months using a stabilizing agent [1,2,12].
4. Microchannel cooling without clogging. Nanofluids are not only a better medium for heat transfer in general but they are also ideal for microchannel applications where high heat loads are needed. The combination of microchannels and nanofluids will provide highly conducting fluids and a large heat

transfer area. This cannot be attained with meso- or micro-particles because they clog microchannels. Nanoparticles, which are only a few hundreds or thousands of atoms long, are orders of magnitude smaller than the microchannels.

5. Reduced chances of erosion. Nanoparticles are very small, and the momentum they can impart to a solid wall is much smaller. This reduces the chances of component erosion such as heat exchangers, pipelines, and pumps.
6. Reduction in pumping power. To increase the heat transfer of conventional fluids by a factor of two, pumping power must usually be increased by a factor of ten. It can be shown that if one can multiply the conductivity by a factor of three, the heat transfer in the same apparatus doubles [1]. The required

increase in the pumping power will be very moderate unless there is a sharp increase in fluid viscosity. Thus, a very large savings in pumping power can be achieved if a large thermal conductivity increase can be brought about with a small volume fraction of particles.

7. Reduced friction coefficient. Nanofluids could effectively decrease friction.

8. Cost and energy saving. Successful employment of nanofluids will result in significant energy and cost savings because heat exchange systems can be made smaller and lighter.

9. Possible spectrum of applications of nanofluids include more efficient flow and lubrication, cooling and heating in new and critical applications like electronics, nuclear, biomedical instrumentation and equipments, transportation and industrial cooling, heat management in various critical applications, as well as environmental control and cleanup, and bio-medical applications.

TYPES OF NANOFLUIDS

The range of potentially useful combinations of nanoparticle and base fluids is enormous. Nanofluids can be classified broadly by the type of particles into four groups: ceramic, pure metallic, alloy, and some allotropes of carbon or carbon-based nanofluids. Different combinations of the above particles and fluids give different nanofluids. Table 2 shows some experimental studies on different kinds of nanofluids.

Ceramic Nanofluids

The first materials tried for nanofluids were ceramic particles, primarily because they were easy to produce and chemically stable in solution. The ceramics are classified into three distinct categories: oxides such as alumina and zirconia, non-oxides such as carbides, nitrides, and silicides, and composites such as combinations of oxides and non-oxides. Each one of these classes can develop unique material properties.

Among different kinds of ceramics, much interest has been shown on oxide nanofluids. The first published report by Masuda *et al.* [8] reported 30% increases in the thermal

conductivity of water with the addition of 4.3 vol. % Al_2O_3 nanoparticles.

Pure Metallic Nanofluids

Although fewer studies of nanofluids containing metal nanoparticles have been carried out than those of containing oxide nanoparticles, the results have been encouraging. Usually, a much higher effective thermal conductivity is exhibited for a nanofluid consisting of a metal than that of containing the same volume fraction of dispersed oxide of that metal [42].

Alloy Nanofluids

Alloying of metals with different metals is a way of developing new materials with better technological usefulness as compared to their parent metals [70]. Studies on alloy nanoparticles revealed that their physical properties differ from what have been observed in bulk samples. There are few reports for alloy nanofluids in the literature [70,72]. Alloy nanofluids may be prepared by mechanical alloying or by the inert gas condensation process.

Carbon-Based Nanofluids

The large intrinsic thermal conductivity of some carbon-based nanostructures, combined with their low densities as compared to metals, make them attractive candidates for using in nanofluids. Examples of carbon-based nanofluids are fullerenes, carbon nanotubes (single-walled nanotubes (SWNTs), multi-walled nanotubes (MWNTs), and ultra-dispersed diamond) in different fluids.

Compared with metal or metal oxide materials, CNTs have higher thermal conductivity. For example, thermal conductivity values for SWNT, double-walled carbon nanotube, and MWNT are $6000 \text{ W m}^{-1} \text{ K}^{-1}$, $3986 \text{ W m}^{-1} \text{ K}^{-1}$, and $3000 \text{ W m}^{-1} \text{ K}^{-1}$, respectively [85].

One of the first studies involving CNT nanofluids was carried out by Choi *et al.* [74]. They measured the effective thermal conductivity of 1.0 vol.% MWNTs dispersed in synthetic poly(α -olefin) oil and reported 160% increase in thermal conductivity. There are some reasons for this anomalous phenomenon. First, the thermal conductivity of CNT is similar to that of graphite and approaches or even exceeds

Table 2. Some Experimental Studies on Different Kind of Nanofluids

Nanoparticle	Ref.	Nanoparticle	Ref.
Ceramic nanofluids		Metallic nanofluids	
SiC	[13]	Ag	[14-20]
Al ₂ O ₃	[8,21-37]	Au	[15,33,38-40]
CeO ₂	[41]	Cu	[26,27,42-48]
CuO	[26,27,29,31-33,41,49-57]	Fe	[36,58-60]
Fe ₂ O ₃	[61]	Ni	[62]
Fe ₃ O ₄	[63,64]		
		Alloy nanofluids	
SiO ₂		Ag-Cu	[70]
TiO ₂		Ag-Al	[72]
ZnO		Al-Cu	[72]
ZrO ₂			
WO ₃			
Carbon-based nanofluids			
CNT	[40,53,57,74-82]		
Diamond	[14,47,74,83]		
Fullerene	[57]		
Graphite	[79]		
Graphene	[84]		

that of natural diamond, the best room-temperature thermal conductor. Second, nanotubes have high aspect ratios.

PREPARATION OF NANOFLUIDS

There are two primary methods to prepare nanofluids: A two-step process in which nanoparticles or nanotubes are first produced as a dry powder. The resulting nanoparticles are then dispersed into a fluid in a second step. Single-step nanofluid processing methods have also been developed.

Two-Step Methods

Several studies, including the earliest investigations [2] of

nanofluids, used a two-step process in which nanoparticles are first produced as a dry powder. This method is more extensively used to produce nanofluids because nanopowders are commercially available nowadays. A variety of physical, chemical, and laser-based methods are available for the production of the nanoparticles to be used for nanofluids [86-92].

One-Step Methods

The nanoparticles may agglomerate during the drying, storage, and transportation process, leading to difficulties in the following dispersion stage of two-step method. Consequently, the stability and thermal conductivity of nanofluid are not ideal. In addition, the production cost is high.

To reduce the agglomeration of the nanoparticles, one-step methods have been developed. There are some ways for preparing nanofluids using this method including direct evaporation condensation [27,93,94], chemical vapour condensation [95], and single-step chemical synthesis.

STABILITY OF NANOFLUIDS

The production of a nanofluid faces some major challenges such as agglomeration of particles in solution due to very strong van der Waals interactions and the rapid settling of particles in fluids. The special requirements for preparation of a nanofluid are durability and stability of suspension with low agglomeration of particles, and no chemical change of the fluid [96].

Stability of a nanofluid is strongly affected by the characteristics of the suspended particles and base fluids such as the particle morphology and the chemical structure of the particles and base fluid [57].

In order to make a stable suspension, one should reduce the density difference between the particles and the fluid, increase the viscosity of the fluid, and make the particles very small to prevent agglomerating [16].

Methods of Improving the Stability of a Nanofluid

To obtain stable nanofluids, several methods such as electrical, physical, or chemical [82] are used. General common methods are:

(1) Controlling the surface charge of the nanoparticles by controlling the pH. The stability of a nanofluid directly links to its electrokinetic properties. Through a high surface charge density, strong repulsive forces can stabilize a well-dispersed suspension [97]. As the pH of the solution departs from the isoelectric point (IEP) of particles, the colloidal particles get more stable [98,99]. The IEP is the concentration of potential controlling ions at which the zeta potential is zero. Thus, at the IEP, the surface charge is zero.

(2) Modifying the surface by addition of some surfactants. This is one of the general methods to avoid sedimentation of nanoparticles. Surfactants can modify the particles-suspending medium interface and prevent aggregation over long time periods. The reason is that the hydrophobic

surfaces of nanoparticles/nanotubes are modified to become hydrophilic and *vice versa*. Selection of suitable surfactants and dispersants depends mainly upon the properties of the solutions and particles. Surfactant molecules adsorbed on the nanoparticle's surface can decrease the surface energy and thus prevent the agglomeration of particles.

Popular surfactants that have been used in literature can be listed as sodium dodecylsulfate [100], sodium dodecylbenzenesulfonate [101], cetyltrimethylammoniumbromide [102], dodecyl trimethylammonium bromide, sodium octanoate [103], and polyvinylpyrrolidone [104].

Adding surfactants restricts the application of nanofluids at high temperatures [105] when the bonding between surfactant and nanoparticles is damaged and hence, the nanofluid loses its stability and sedimentation of nanoparticles occurs [106].

(3) Using ultrasonic vibration. Ultrasonic bath, processor, and homogenizer are powerful tools for breaking down the agglomerations in comparison with other methods like magnetic and high shear stirrer as experienced by researchers [97].

Each of the above techniques or combination of them such as simultaneous use of ultrasonic agitation and addition of surfactants are sometimes used to minimize particle aggregation and to improve dispersion behavior.

The best way to produce a stable suspension may be a single-step method where instead of nanoparticles, nanofluids are produced directly, thus reducing the chance of agglomeration [82].

Stability Evaluation

The Derjaguin-Landau-Verwey-Overbeek (DLVO) theory [107,108] for colloidal interactions dictates that a colloidal system will remain stable if and only if the columbic repulsion, arising from the net charge on the surfaces of the particles in a colloid, is greater than the van der Waals forces. When the reverse is true, the colloidal particles will cluster together and form flocculates and aggregates.

Although the stability of nanofluids is very important for their applications, there are limited studies on estimating the stability of a suspension. There are some ways for evaluating the stability of a nanofluid:

(1) Measuring the zeta potential which is the overall charge that a particle acquires in a specific medium and is a good

indicator for the colloidal stability of a nanofluid [109]. The higher the absolute zeta potential, the stronger the coulombic repulsion between the particles, and therefore, the lower impact of the van der Waals forces on the colloid. Zeta potential measurement is one of the most critical tests to validate the quality of the nanofluids stability *via* a study of its electrophoretic behavior [110].

(2) Measuring particle size distribution by transmission electron microscopy (TEM) or light scattering methods. The nanofluid becomes more stable when nanoparticles have narrow particle size distribution.

(3) UV-Vis spectrophotometric measurements. UV-Vis analysis is an efficient way to evaluate the stability of nanofluids. If nanomaterials dispersed in fluids have characteristic absorption bands in the wavelength range of 190-1100 nm, it is an easy and reliable method to evaluate the stability of nanofluids using UV-Vis spectral analysis. The variation of supernatant particle concentration of nanofluids with sedimentation time can be obtained by the measurement of absorption of nanofluids because there is a linear relation between the supernatant nanoparticle concentration and the absorbance of suspended particles. The outstanding advantage of UV-Vis spectral analysis compared to other methods is that it can present the quantitative concentration of nanofluids [111]. The first work to quantitatively characterize colloidal stability of the dispersions of CNT by UV-Vis scanning spectrophotometric measurements was reported by Jiang *et al.* [100]. However, this method is unsuitable for high concentration of nanofluids because these dispersions are too dark to differentiate the sediment visibly [97].

(4) Cryogenic electron microscopy (Cryo-TEM, Cryo-scanning electron microscopy) is another efficient method to distinguish the shape, size, distribution, and aggregation of nanoparticles in a fluid if the microstructure of nanofluids is not changed during cryoation [112].

PHYSICAL PROPERTIES OF NANOFUIDS

Up to now, the thermal conductivity, viscosity, density, specific heat, and surface tension of the nanofluids have been investigated.

Thermal Conductivity

Among all the physical properties of nanofluids, the

thermal conductivity is the most complex and for many applications the most important one [113].

By suspending some of the nanoparticles in heating or cooling fluids, the heat transfer performance of the fluid can be improved significantly. The main reasons of such enhancement may be listed as follows [12]:

1. The suspended nanoparticles increase the surface area and the heat capacity of the fluid.
2. The suspended nanoparticles increase the effective (or apparent) thermal conductivity of the fluid.
3. The interaction and collision between particles and fluid are intensified.
4. The mixing fluctuation and turbulence of the fluid are intensified.
5. The dispersion of nanoparticles flattens the transverse temperature gradient of the fluid.

Some experimental studies on thermal conductivity of nanofluids are summarized in Table 3.

Important parameters. A nanofluid is a mixture of liquid and nanoparticles, and several factors influence on its thermal conductivity. From the experimental results of many researchers, it is known that the thermal conductivity of nanofluids depends on many parameters including:

1. Thermal conductivity of base fluid

Moosavi *et al.* [71] measured some physicochemical properties including thermal conductivity, viscosity, and surface tension of ZnO nanoparticles in ethylene glycol and glycerol as base fluids. They found that the enhanced thermal conductivity ratio decreases with increasing thermal conductivity of the base fluid.

2. Thermal conductivity of nanoparticles

The thermal conductivity of a nanofluid containing a metal is greater than that of oxide of that metal at the same conditions [132].

3. Volume fraction

The thermal conductivity of a nanofluid is strongly dependent on the nanoparticle volume fraction [12]. Yeganeh *et al.* [83] measured thermal conductivity enhancements of nanodiamond particles suspended in deionized water with different volume fractions in the range from 0.8% to 3%. They observed the highest enhancement in the thermal conductivity (7.2%) for a volume fraction of 3%.

Abareshi *et al.* [64] prepared magnetic nanofluids by dispersing the Fe₃O₄ nanoparticles in water in the presence of

Table 3. Summary of Some Experimental Studies on Thermal Conductivity of Nanofluids

Nanoparticle	Base fluid	Size of nanoparticles	Particle concentration	Findings	Ref.
CNT	Oil	D=25 nm, L=50 μm	$\Phi = 0.3\text{-}1\%$	Thermal conductivity was anomalously greater than theoretical predictions and is nonlinear with nanotube loadings.	[74]
Nitric acid treated CNT	Water/ethyleneglycol/decene	D=15 nm, L=30 μm	$\Phi = 0.3\text{-}1.5\%$	Thermal conductivity enhanced with increasing the volume fraction. The enhanced thermal conductivity ratios are reduced with the increasing thermal conductivity of the base fluid.	[76]
Fe	Ethylene glycol	10 nm	$\Phi = 0.55\%$	18% increase in thermal conductivity was observed.	[59]
TiO ₂ (rod-shaped)	Water	D=10 nm, L=40 nm	$\Phi = 0.5\text{-}5\%$	Maximum enhancement in thermal conductivity was 33%.	[65]
TiO ₂ (spherical shaped)		15 nm		Maximum enhancement in thermal conductivity was 30%.	
Au	Toluene	1.65 nm	$\Phi = 0.003\%$		
Al ₂ O ₃	Water	20 nm	$\Phi_w = 10\text{-}40\%$	Thermal conductivity increased with an increase in the particle concentration and particle thermal conductivity.	[114]
TiO ₂	Water	40 nm	$\Phi = 0.5\text{-}2.5\%$		
CuO	Water	33 nm	$\Phi = 0.5\text{-}4.5\%$		
Al ₂ O ₃	Water	30 nm	$\Phi = 0.01\text{-}0.3\%$	Thermal conductivities of the dilute Al ₂ O ₃ -water nanofluids increase nearly linearly with the concentration.	[115]
Al ₂ Cu	Water/ethylene glycol	30-105 nm	$\Phi = 1\text{-}2\%$	The higher the volume percent of nanoparticles, the greater was the effective thermal conductivity and the smaller the dispersoid size, the greater is the enhancement in the thermal conductivity.	[116]
Ag ₂ Al		30-120 nm	$\Phi = 1\text{-}2\%$		

Table 3. Continued.

Nanoparticle	Base fluid	Size of nanoparticles	Particle concentration	Findings	Ref.
Al ₂ O ₃	Water	15-50 nm	$\Phi_w = 0.02-0.15\%$	For weight fraction of 0.15 wt%, thermal conductivity was enhanced by up to 10.1%.	[117]
Acid treated CNT	Silicone oil	D= 30–50 nm, L=20 μ m	$\Phi = 0.002, 0.0054, 0.01\%$	Thermal characteristics of nanofluids might be manipulated by means of controlling the morphology of CNT.	[118]
TiO ₂	Water	21 nm	$\Phi = 0.2-2\%$	Thermal conductivity of nanofluids increased as the particle concentrations increased and are higher than the values of the base liquids.	[119]
Al ₂ O ₃	Water	43 nm	$\Phi = 0.33-5\%$	Thermal conductivity of nanofluids increased with the nanoparticle volume concentration.	[120]
Al ₂ O ₃	Water	20, 50, 100 nm	$\Phi_w = 0.5-2\%$	Shrinkage of particle size enhanced the thermal conductivity ratio of nanofluid.	[121]
Diamond	Water	10 nm	$\Phi = 0.8-3\%$	The highest observed enhancement in the thermal conductivity was 7.2% for a volume fraction of 3%	[83]
CuO	Gear oil	40 nm	$\Phi = 0.5-2.5\%$	An enhancement in thermal conductivity of 10.4% with 2.5% volume fraction of CuO nanoparticle loading was observed	[122]
SiC	Water	100 nm	$\Phi = 0.001-3\%$	Thermal conductivity of SiC/DIW nanofluids increases with an increase of volume fraction.	[123]
γ -Al ₂ O ₃	Carboxymethyl cellulose aqueous solution	25 nm	$\Phi = 0.1-4\%$	Thermal conductivity of nanofluids is higher than the one of the base fluid and the increase in the thermal conductivity varies exponentially with the nanoparticle concentration.	[124]
TiO ₂		10 nm			
CuO		30-50 nm			

Table 3. Continued.

Nanoparticle	Base fluid	Size of nanoparticles	Particle concentration	Findings	Ref.
AlN	Ethylene glycol/propylene glycol	50 nm	$\Phi = 0.01-0.10\%$	At a volume fraction of 0.1, the thermal conductivity enhancement ratios are 38.71% and 40.2%, respectively, for ethylene glycol and propylene glycol as the base fluids.	[125]
CuO	Water	50 nm	$\Phi = 0.025\%$, 0.05% 0.1%	An enhancement in thermal conductivity over the base fluid was witnessed for the tested temperature and volume fraction	[126]
Fe ₃ O ₄	Water	10 nm	$\Phi = 5\%$	A ferrofluid with 5.0% volume fraction of nanoparticles enhanced the thermal conductivity more than 200% at maximum value.	[127]
TiO ₂ Al ₂ O ₃	Water/ethylene glycol-water mixture	21 nm 120	$\Phi = 0-8\%$	Thermal conductivity of nanofluids increased with respect to the base fluid and increased with increasing concentration and temperature.	[128]
Polyaniline nanofibers	Water	D=80 nm, L=2 μ m	$\Phi = 0.08, 0.16, 0.24\%$	Maximum thermal conductivity enhancement ratio was 140% with 0.24 vol% of nanofibers loading.	[129]
CNT	Water	D=1-20 nm, L=10 μ m	$\Phi_w = 0.25\%$	As the number of nanotube wall increased, thermal conductivity decreased.	[130]
Al ₂ O ₃ /SiO ₂	Methanol	40-50 nm	$\Phi = 0.005-0.5\%$.	Thermal conductivity increases with an increase of the nanoparticle volume fraction, and the enhancement is observed to be 10.74% and 14.29% over the basefluid at the volume fraction of 0.5vol% for Al ₂ O ₃ and SiO ₂ nanoparticles.	[131]

D: Diameter of nanostructures; L: length of nanotubes; Φ : volume concentrations; Φ_w : mass fractions of particles T: temperature.

tetramethyl ammonium hydroxide as a dispersant. They found that the thermal conductivity ratio of the nanofluids increases with increase in volume fraction. The highest enhancement of thermal conductivity was 11.5% in the nanofluid of 3 vol% of nanoparticles at 40 °C.

4. Size of nanoparticles

Nanofluids containing smaller particles show greater enhancement of thermal conductivity than that of larger particles. The stochastic motion of nanoparticles could be a probable explanation of the thermal conductivity enhancement. This is because smaller particles are more easily to mobilize and cause a higher level of stochastic motion.

Teng *et al.* [121] examined the effect of particle size on the thermal conductivity ratio of alumina/water nanofluids. The results of their work indicated that shrinkage of particle size enhances the thermal conductivity ratio of nanofluids.

5. Shape of the nanoparticles

There are mainly two particle shapes investigated in nanofluid research; spherical and cylindrical particles. Nanofluids with spherical shape nanoparticles exhibit a smaller increase in thermal conductivity compared with the nanofluids having cylindrical (nano-rod or tube) nanoparticles [65] because cylindrical particles usually have a large length-to diameter ratio [133]. Murshed *et al.* [65] prepared nanofluids by dispersing TiO₂ nanoparticles in rod-shapes of 10 nm × 40 nm (diameter by length) and in spherical shapes of 15 nm in deionized water and compared the thermal conductivity of resulting nanofluids. They showed that particle shape could affect the enhancement of thermal conductivity so that the increase in thermal conductivity for nanofluid with rod-shape nanoparticles is larger than those of with spherical shaped particles.

6. The effect of pH

The number of studies regarding the pH of nanofluids is limited, compared to the other parameters. Karthik *et al.* [126] studied the influence of pH range including the isoelectric point on the thermal conductivity of CuO-deionized water nanofluids. They observed that thermal conductivity ratio with pH increases and reaches to a maximum close to the isoelectric point and decreases as pH further increases.

7. Aspect ratio

Nanoparticles with a high aspect ratio such as CNTs or

nanorods greatly increase the thermal conductivity of the nanofluids.

8. Temperature

A potentially important development in the field of nanofluids is the strong temperature effect on thermal conductivity. Das *et al.* [21] systematically discussed the relationship between thermal conductivity and temperature for nanofluids, noting significant increases of thermal conductivity with temperature.

Lee *et al.* [2] measured the thermal conductivity of oxide nanofluids over the temperature range of 21-50 °C. The results revealed an almost threefold increase in conductivity enhancement for copper oxide and alumina nanofluids. These findings have revolutionized the application of nanofluids because they indicate a much larger thermal conductivity at the elevated temperatures and even more attractive as cooling fluid for devices with high energy density where the cooling fluid is likely to work at a temperature higher than the room temperature. These results also open up the possibility that nanofluids could be employed as “smart fluids” sensing hot spots and providing more rapid cooling in those regions.

9. Effect of clustering

The clustering effect is always present in nanofluids and is an effective parameter in thermal conductivity. Hong *et al.* [134] investigated this effect for Fe (10 nm)/ethylene glycol nanofluids. The thermal conductivity was determined as a function of ultrasonic vibration time between 0 min and 70 min. It was observed that thermal conductivity ratio increases with increasing vibration time. For longer vibration times, the increase in conductivity ratio was smaller than that of the shorter vibration times. Furthermore, the variation of thermal conductivity of nanofluid with time, after applying the vibration, was investigated and it was found that thermal conductivity decreases as time progresses. Variation of average size of clusters was also determined as a function of time, after applying the vibration, and the results showed that cluster size increases with time. The final conclusion was that the size of the clusters formed by the nanoparticles has a major influence on the thermal conductivity. In addition, the variation of thermal conductivity ratio of the Fe/ethylene glycol nanofluid with particle volume fraction is nonlinear. This behavior is due to the fact that nanoparticles in the

nanofluids with high volume fractions form clusters at a higher rate.

Measurement of Thermal Conductivity of Nanofluids

To measure the thermal conductivity of nanofluids, transient hot wire (THW) [135], transient plane source (TPS) [129], temperature oscillation (TO) [136], steady-state parallel plate techniques [137], and optical methods [113] have been reported.

Transient hot wire method. The THW technique was introduced in 1974 [135]. It is the most popular dynamic method. In this technique, a cylindrical fluid volume is heated electrically using a current-carrying metallic wire stretched along the axis of the fluid volume. The differential temperature rise of the wire is calculated based on the changes in the electrical resistance of the wire at different times and then plotting it against the natural logarithm of the time. This plot is expected to have a linear region, from the slope of which the thermal conductivity of the fluid can be calculated.

The advantages of the THW method are [138]:

1. Capability of the experimentally eliminating convective error
2. Fast measurement time compared with other techniques
3. Obtaining reliable data

Because in general nanofluids are electrically conductive, it is difficult to apply the ordinary THW technique directly. A modified hot-wire cell and electrical system was proposed by Nagasaka and Nagashima [139] by coating the hot wire with an epoxy adhesive which has excellent electrical insulation and heat conduction.

Transient plane source. TPS method is the modified version of THW technique for heat transfer measurements. TPS unit works using temperature coefficient of nickel sensor resistance. The bath temperature value can match with temperature of sample near the sensor. This helps in measuring precise thermal conductivity values at exact temperatures. Many materials have different thermal conductivity values at different temperatures so precise measurement of the thermal conductivity at certain temperatures minimizes the uncertainty. The TPS element behaves both as the temperature sensor and the heat source. The TPS method uses the Fourier law of heat conduction as a fundamental principle for measuring the thermal conductivity. The thermal conductivity of the nanofluid is determined by

measuring the resistance of the probe.

Advantages of using this method are (1) fast measurements, (2) measurements in wide ranges of thermal conductivities (from 0.02 to 200 W m⁻¹ K⁻¹, with 2% uncertainty), (3) no need to sample preparation and (4) flexible sample sizes.

The experimental setup (as shown in Fig. 6 reference [140]) comprises of thermal constants analyzer, a vessel, a constant temperature bath, and a thermometer. The probe of the thermal constant analyzer is immersed vertically in the vessel containing the nanofluid. The vessel is placed in the constant temperature bath and the thermometer is immersed in the vessel to measure the temperature of the nanofluid. The thermal conductivity of the nanofluid is determined by measuring the resistance of the probe [140].

Temperature oscillation technique. TO was introduced by Santucci and co-workers [136]. It consists of filling a cylindrical volume with the fluid. The thermal conductivity is measured by applying an oscillating temperature boundary condition at the two ends of the cylinder. By measuring the amplitude and phase of the temperature oscillation, the fluid thermal conductivity could be calculated [141]. The simplicity of the temperature oscillation technique makes it more appealing.

Steady-state parallel plate method. In steady-state method, a fluid layer is subjected to a stationary temperature gradient while the heat flow is measured as a function of this gradient. Two steady-state geometries have found wide acceptance: concentric cylinders and parallel plates [137]. In the first method, the fluid is enclosed between two concentric cylinders in horizontal or vertical orientation, and heat is generated in the inner cylinder. In the second method, the fluid is enclosed between two parallel plates and heat is generated in the upper plate. The possibility of convection is also present in this steady state method but the parallel-plate method offers the advantage that the heat is developed from above and thus convection develops less easily.

Optical methods. Optical methods have been proposed as non-invasive techniques for thermal conductivity measurements to improve accuracy. Indeed, because the "hot wire" is a combination of heater and thermometer, interference is unavoidable. In optical techniques, detector and heater are always separated from each other providing potentially more accurate data. Additionally, measurements are completed

within several microseconds, *i.e.*, much shorter than reported THW measurement times of 2 to 8 s, so that natural convection effects are avoided [113].

Models for Predicting the Effective Thermal Conductivity of Nanofluids

There are no theoretical formulas currently available to predict the thermal conductivity of nanofluids satisfactorily. A variety of theoretical models have been developed to predict the effective conductivity of nanofluids.

Classical Models. Pls transfer this line to line 1072 theoretical models have been derived to predict the thermal conductivity of suspensions. For example, for spherical particles, the models of Maxwell [5], Jeffrey [142], and Davis [143] and for nonspherical particles, the model of Hamilton and Crossover [144] have been widely used. We briefly discuss some of the most widely used models.

Maxwell model. The Maxwell model [5] was proposed for solid-liquid mixtures with relatively large particles. According to Maxwell model the effective thermal conductivity of suspensions depends on the thermal conductivity of spherical particles, base liquid, and the volume fraction of the solid particles:

$$\kappa_{eff} = \frac{\kappa_p + 2\kappa_f + 2(\kappa_p - \kappa_f)\phi}{\kappa_p + 2\kappa_f - (\kappa_p - \kappa_f)\phi} \kappa_f \quad (1)$$

where k_f and k_p are the thermal conductivities of the base fluid and nanoparticles, respectively, and ϕ is the volume fraction. Maxwell's model predicts that the effective thermal conductivity of suspensions containing spherical particles increases with the volume fraction of the solid particles. When the particle concentration is sufficiently high, the Maxwell model fails to provide a good match with the experimental results.

Jeffrey model. The Maxwell equation takes into account only the particle volume concentration and the thermal conductivities of particle and liquid. Jeffrey model [142] includes the effects of particle-particle interactions as well:

$$\frac{\kappa_{eff}}{\kappa_f} = 1 + 3\beta\phi + (3\beta^2 + \frac{3\beta^3}{4} + \frac{9\beta^3}{16} \frac{\alpha + 2}{2\alpha + 3} + \frac{3\beta^4}{64} + \dots)\phi^2 \quad (2)$$

where α is the thermal conductivity ratio, k_p/k_f , and β is defined as:

$$\beta = \frac{\alpha - 1}{\alpha + 2} \quad (3)$$

Equation (2) is accurate up to the order of ϕ^2 . The higher-order terms represent pair interactions of randomly dispersed spheres. The ratio k_{eff}/k_f is called thermal conductivity enhancement.

Davis model. As two previous models, Davis model [143] is applied to spherical suspensions and has the form:

$$\frac{\kappa_{eff}}{\kappa_f} = 1 + \frac{3(\alpha - 1)}{[\alpha + 2 - (\alpha - 1)\phi]} [\phi + f(\alpha)\phi^2 + O(\phi^3)] \quad (4)$$

$f(\alpha)$ is a function of α , $f(\alpha) = 2.5$ for $\alpha = 10$ and $f(\alpha) = 0.5$ for $\alpha = \infty$.

Jeffery model is accurate up to the order of ϕ^2 .

Hamilton and Crossover model. Hamilton-Crosser model [117] is an important model for explaining thermal conductivity enhancement in particle shape dependent cases. Hamilton and Crosser proposed the following model to predict the effective thermal conductivity for liquid-solid mixtures for non-spherical particles:

$$\kappa_{eff} = \frac{\kappa_p + (n-1)\kappa_f - (n-1)(\kappa_f - \kappa_p)\phi}{\kappa_p + (n-1)\kappa_f + (\kappa_f - \kappa_p)\phi} \kappa_f \quad (5)$$

where n is the empirical shape factor given by $n = 3/\psi$, and ψ is the particle sphericity, defined as the ratio of the surface area of a sphere with volume equal to that of the particle, to the surface area of the particle. Comparison of Eqs. (1) and (5) reveals that Maxwell's model is a special case of the Hamilton and Crosser model for sphericity equal to one. The previous models do not consider the effect of particle sizes. However, the thermal conductivities predicted by the Hamilton-Crosser model are much lower than the experimentally measured conductivities.

The classical models originated from continuum formulations. They typically involve only the particle size/shape and volume fraction and assume diffusive heat

transfer in both fluid and solid phases. Although they can give good predictions for micrometer or larger-size multiphase systems, the classical models usually underestimate the enhancement of thermal conductivity increase of nanofluids as a function of volume fraction [113].

Recent Models

Recently, many theoretical studies have been made and several mechanisms have been proposed in order to explain the anomalous thermal conductivity enhancement obtained with nanofluids. Based on the effective medium approximation and the fractal theory for the description of nanoparticle cluster and its radial distribution, a method for predicting the effective thermal conductivity of nanofluid was established by Wang *et al.* [145]. They took the size effect and the surface adsorption of nanoparticles into considerations. It can be expressed as:

$$\frac{\kappa_{eff}}{\kappa_f} = \frac{(1-\phi) + 3\phi \int_0^{\infty} \frac{\kappa_{cl}(r)n(r)}{\kappa_{cl}(r) + 2\kappa_f} dr}{(1-\phi) + 3\phi \int_0^{\infty} \frac{\kappa_f n(r)}{\kappa_{cl}(r) + 2\kappa_f} dr} \quad (6)$$

where $\kappa_{cl}(r)$ is the effective thermal conductivity of clusters and $n(r)$ is the radius distribution function.

To lower the difference between the experimental data and the predicted values by the previous models, it is necessary to develop a new model using the effective volume fraction. From the viewpoint of the mechanism of heat transfer in nanofluids, the enhancement of thermal conductivity may be due to the effects of liquid layer on the particles and the effects of Brownian motion of nanoparticles [14]. The interface liquid has a strong interaction with particles that makes the interfacial liquid layer a more ordered structure. The interfacial-layer liquid has a higher thermal conductivity than that of the bulk phase liquid. Since the interface between solid and liquid is regarded as a very thin nanolayer and has semi-solid material properties, the effective volume of nanoparticles can be estimated using this nanolayer. The effect of interface on particles volume is not important in the suspension with micrometer particles but it is very significant in the nanofluid. Yu and Choi [146] suggested that the effective volume fraction of particles is

$$\phi_{eff} = \frac{4}{3} \pi (r+h)^3 = \phi(1+\beta)^3 \quad (7)$$

and the effective thermal conductivity is

$$\kappa_{eff} = \kappa_f \left[\frac{\kappa_p + (n-1)\kappa_f - \phi_{eff}(n-1)(\kappa_f - \kappa_p)}{\kappa_p + (n-1)\kappa_f + \phi_{eff}(\kappa_f - \kappa_p)} \right] \quad (8)$$

where t is the thickness of nanolayer and β is the ratio of the nanolayer thickness, t , to the particle diameter, d_p , ($\beta = t/d_p$). The thermal conductivity of nanofluid can be estimated from this effective volume fraction using the previous semi-empirical models. They suggested that the thickness of the liquid layer on nanoparticles is about 3 nm. However, since the thickness of liquid layer varies with the surface structure and shape of particles, it must be estimated more precisely.

Xuan *et al.* [147] studied the thermal conductivity of nanofluids by considering Brownian motion and clustering of nanoparticles. He proposed an equation to predict the thermal conductivity of nanofluids:

$$\frac{k_{eff}}{k_f} = \frac{k_p + 2k_f - 2\phi(k_f - k_p)}{k_p + 2k_f + \phi(k_f - k_p)} + \frac{\rho_p \phi c_{p,p}}{2k_f} \sqrt{\frac{k_B T}{3\pi r_{cl} \mu_f}} \quad (9)$$

r_{cl} is the apparent radius of the nanoparticle clusters, which should be determined by experiment. μ_f is the dynamic viscosity of the base fluid. The first term on the right-hand side of Eq. (9) is the Maxwell model for thermal conductivity of suspensions of solid particles in fluids. The second term on the right-hand side of Eq. (9) adds the effect of the random motion of the nanoparticles into account.

Bhattacharya *et al.* [148] used Brownian dynamics simulation to determine the effective thermal conductivity of nanofluids, by considering the Brownian motion of the nanoparticles. Effective thermal conductivity of the nanofluid was defined as:

$$k_{eff} = \phi k'_p + (1-\phi)k_f \quad (10)$$

where k'_p is not simply the bulk thermal conductivity of the nanoparticles but also includes the effect of the Brownian motion of the nanoparticles on the thermal conductivity.

Jang and Choi [149] modeled the thermal conductivity of

nanofluids by considering the effect of Brownian motion of nanoparticles. The proposed model is a function of not only thermal conductivities of the base fluid and nanoparticles but it also depends on the temperature and size of the nanoparticles. Energy transport in nanofluids was considered to consist of four modes; heat conduction in the base fluid, heat conduction in nanoparticles, collisions between nanoparticles (due to Brownian motion), and micro-convection caused by the random motion of the nanoparticles. Among these, the collisions between nanoparticles were found to be negligible when compared to other modes. As a result of the consideration of the three remaining modes, the following expression was presented:

$$k_{eff} = k_f(1-\phi) + k_p^* \phi + 3c_1 \frac{d_f}{d_p} k_f Re_d^2 Pr_f \phi \quad (11)$$

where c_1 is a proportionality constant, d_f the diameter of the fluid molecules, Pr_f Prandtl number of base fluid, and k_p^* is defined so that it also includes the effect of the Kapitza resistance.

Koo and Kleinstreuer [150] considered the effect of thermal conductivity enhancement due to both Brownian motion and static contribution on the effective thermal conductivity of nanofluids. This model takes into account the effects of the particle dynamics. For the calculation of thermal conductivity of static part (K_{static}), Maxwell's model is used (Eq. (1)). For contribution of Brownian motion of particles, $K_{Brownian}$ was considered together with the effect of fluid particles moving with nanoparticles around them. As a result, the following expression was proposed:

$$k_{Brownian} = 5 \times 10^4 \gamma \phi \rho_f c_{p,f} \sqrt{\frac{k_B T}{\rho_p d_p}} f \quad (12)$$

where ρ_p and ρ_f are the density of nanoparticles and base fluid, respectively. $c_{p,f}$ is specific heat capacity of the base fluid. In the analysis, the interactions between nanoparticles and fluid volumes moving around them were not considered and an additional term, γ was introduced to take that effect into account. Koo and Kleinstreuer indicated that this term becomes more effective with increasing volume fraction. Another parameter, f , was introduced to the model in order to

increase the temperature dependency of the model. Both f and γ were determined by utilizing available experimental data. It is difficult to determine theoretical expressions for f and γ due to the complexities involved and this can be considered as a drawback of the model.

Xue and Xu [151] presented another theoretical study for the effective thermal conductivity of nanofluids. In their derivation, nanoparticles were assumed to have a liquid layer around them with a given specific thermal conductivity. The resulting implicit expression for thermal conductivity of nanofluids is:

$$\left(1 - \frac{\phi}{\alpha}\right) \frac{k_{eff} - k_f}{2k_{eff} + k_f} + \frac{\phi(k_{eff} - k_{lr})(2k_{lr} + k_p) - \alpha(k_p - k_{lr})(2k_{lr} + k_{eff})}{\alpha(2k_{eff} + k_{lr})(2k_{lr} + k_p) - 2\alpha(k_p - k_{lr})(k_{lr} + k_{eff})} = 0 \quad (13)$$

where subscript lr refers to nanolayer. α is defined as:

$$\alpha = \left(\frac{d_p}{d_p + t}\right)^3 \quad (14)$$

By considering the effect of the interfacial layer at the solid particle/liquid interface, Leong *et al.* [152] developed a model for determining the effective thermal conductivity of nanofluids.

$$k_{eff} = \frac{(k_p - k_{lr})\phi k_{lr} [2\beta_2^3 - \beta^3 + 1] + (k_p + 2k_{lr})\beta_2^3 [\phi\beta^3(k_{lr} - k_f) + k_f]}{\beta_1^3(k_p + 2k_{lr}) - (k_p - k_{lr})\phi[\beta_2^3 + \beta^3 - 1]} \quad (15)$$

where $\beta_1 = t/2d_p$. This model accounts for the effects of particle size, interfacial layer thickness, volume fraction, and thermal conductivity. If there is no interfacial layer at the particle/liquid interface *i.e.*, $k_{lr} = k_f$ and $\beta_1 = \beta = 1$, Eq. (15) reduces to the Maxwell model (Eq. (1)).

Another study regarding the effect of nanolayers was made by Sitprasert *et al.* [153]. They modified the model proposed by Leong *et al.* [152] by taking the effect of temperature on the thermal conductivity and thickness of nanolayer into account. Sitprasert *et al.* provided the following relation for the determination of nanolayer thickness:

$$t = 0.01(T - 273)d_p^{0.35} \quad (16)$$

After the determination of nanolayer thickness, thermal conductivity of the nanolayer should be found according to the expression:

$$k_{lr} = C \frac{t}{r_p} k_f \quad (17)$$

where C is 30 and 110 for Al_2O_3 and CuO nanoparticles, respectively.

Yang and Du [154] proposed a thermal conductivity model which includes the effects of the interfacial layer formed by the surfactant and liquid molecules upgrading Leong *et al.* model [152]. Based on the analysis of dispersion type, the thickness of the interfacial layer is defined by the length of the surfactant molecule for nanofluid under monolayer adsorption dispersion and double lengths of the surfactant molecule for nanofluid under electric double layer adsorption dispersion. The model for cylindrical coordinates is as follows (nanofluids containing nanotubes):

$$k_{eff} = \frac{(k_p - k_{lr})\phi k_{lr} [2\beta_1^2 - \beta^2 + 1] + (k_p + k_{lr})\beta_1^2 [\phi\beta^2 (k_{lr} - k_f) + k_f]}{\beta_1^2 (k_p + 2k_{lr}) - (k_p - k_{lr})\phi[\beta_1^2 + \beta^2 - 1]} \quad (18)$$

Concerning theories/correlations which try to explain thermal conductivity enhancement for all nanofluids, not a single model can predict a wide range of experimental data [113].

Potential Mechanisms of the Enhancement of Heat Conduction in Nanofluids

Different authors proposed different mechanisms of heat transfer in nanofluids [145,146,149,155-159]. The proposed mechanisms for the anomalous enhancement discussed in the literature are:

1. Motion of the nanoparticles
2. Liquid layering at liquid/particle interface
3. Nature of heat transport in nanoparticles
4. Effects of nanoparticle clustering
5. Surface charge state
6. Coupled transport

Because of the complexity and contradiction in nanofluids, the research community has not reached a solid consensus on the mechanisms.

Motion of the nanoparticles. The energy exchange in

direct nanoparticle-nanoparticle contact arising from particle collisions in the nanofluid could result in an enhancement of the thermal conductivity. Such collisions arise from the motion of the nanoparticles. Furthermore, even without collisions the Brownian motion of particles might enhance thermal conductivity. The movement of nanoparticles due to Brownian motion is too slow to transport significant amounts of heat through a nanofluid. Although, Brownian motion cannot directly result in an enhancement of the thermal transport properties, it could have an important indirect role in producing particle clustering that could significantly enhance thermal conductivity [160].

Liquid layering at liquid/particle interface. Liquid molecules are known to form ordered layered structures at solid surfaces and these interfacial layers have different thermophysical properties from the bulk liquid and solid particles. Because of the ordered structure of the nanolayer, it is expected to have higher thermal conductivity than the bulk liquid [161]. Although, the presence of an interfacial layer may play a role in heat transport, it is not likely to be solely responsible for the enhancement of thermal conductivity [162].

Nature of heat transport in nanoparticles. Macroscopic theories assume that heat is transported by diffusion. In crystalline solids, heat is carried by phonons, that is, by the propagation of lattice vibrations. Such phonons are created at random, propagate in random directions and are scattered by each other or by defects. When the size of the nanoparticles in a nanofluid becomes less than the phonon mean-free path, phonons no longer diffuse across the nanoparticle but move ballistically without any scattering. Without going into the details of ballistic heat transport, it is difficult to envision how ballistic phonon transport could be more effective than a very-fast diffusion phonon transport [160].

Effects of nanoparticle clustering. If particles cluster into percolating networks, they would create paths of lower thermal resistance and thereby have a major effect on the effective thermal conductivity. However, clustering to the extent that solid agglomerates span large distances is unlikely; moreover any such large clusters would most likely settle out of the fluid.

A further dramatic increase of thermal conductivity can take place if the particles do not need to be in physical contact

but just close enough to allow rapid heat flow between them. Such liquid-mediated clusters exhibit a very low packing fraction and thus a very large effective volume and, in principle, are capable of explaining the unusually large experimentally observed enhancements of thermal conductivity [162]. However, clustering may exert a negative effect on heat transfer enhancement, particularly at low volume fractions, by settling small particles out of the liquid and creating large regions of particle-free liquid with high thermal resistance.

Surface charge state. Since the pH of nanofluids strongly affects the performance of the thermal conductivity, the surface charge is a basic parameter that is primarily responsible for the enhancement of thermal conductivity of the nanofluids [99].

Coupled transport. Normally in a nanofluid system, there are two or more transport processes that occur simultaneously. Examples are the heat conduction in dispersed and continuous phases, mass transport, and chemical reactions either among the nanoparticles or between the nanoparticles and the base fluid. These processes may couple and cause new induced effects of flows occurring without or against its primary thermodynamic driving force, which may be a gradient of temperature, or chemical potential, or reaction affinity. Two classical examples of coupled transport are the Soret effect (also known as thermodiffusion) in which directed motion of particles or macromolecules is driven by thermal gradient and the Dufour effect [163] that is an induced heat flow caused by the concentration gradient. While the coupled transport is well recognized to be very important in thermodynamics, it has not been well appreciated yet in the nanofluid community [164].

Rheological Property

Rheology is the science of the deformation and flow of matter. The rheological behavior of a nanofluid is an important attribute in its applications. The study of the rheological behavior of a nanofluid also helps to understand the structure of the nanofluid.

The quantities measured in rheological investigations are forces, deflections, velocities, and viscosities. Viscosity is an important parameter in designing nanofluids for flow and heat transfer applications in thermal devices or systems such as heat exchangers or cooling systems because the resulting pumping power depends on the viscosity. In a laminar flow,

the pressure drop is directly proportional to the viscosity. Furthermore, convective heat transfer coefficient is influenced by viscosity. Hence, viscosity is as important as thermal conductivity in engineering systems involving fluid flow [165]. A summary of literatures about the viscosity of nanofluids for different parameters is listed in Table 1 of Ref. [166].

Important parameters affecting viscosity of nanofluids. Some parameters like temperature, particle size and shape, particle size distribution, shear rate, surfactant, and volume concentrations have great effects on the viscosity of nanofluid [167].

Effect of temperature. As temperature increases, the intermolecular interactions between nanoparticles and fluid as well as the molecules of fluid weaken. Hence, the viscosity of the nanofluid decreases with increasing the temperature. Namburu *et al.* [168] investigated the rheological properties of copper oxide nanoparticles suspended in ethylene glycol and water mixture. They carried out the experiments over temperatures ranging from -35 °C to 50 °C and showed that the relative viscosity diminishes as temperature increases. The shear viscosity is found to depend strongly on temperature and all the data were found to fit the following equation very well [169]:

$$\ln \eta = A + 1000 \frac{B}{T + C} \quad (19)$$

where T is the absolute temperature, and A , B , and C are constants. Equation (19) is originated from $\ln \eta = A + B/T$, which, known as Andrade equation [170]. The Andrade equation was then improved by introducing a third parameter, C , to give Eq. (19) by Vogel [171], Tamman and Filchers [172]. The equation is also called VTF equation. The three parameters in Eq. (19) have clear physical meanings: A is the value of $\ln \eta$ at the infinite temperature, B corresponds to the energy barrier associated with the so-called 'cage' confinement due to the close packing of liquid molecules, implying any structural rearrangement of liquid molecules would need to overcome the energy barrier, and C represents the temperature at which viscosity becomes infinite. It is also called zero-mobility temperature at which the free volume or configurational entropy of the liquid would vanish.

Goharshadi and Hadadian [173] studied the rheological

properties of ZrO₂/ethylene glycol nanofluid. They showed that viscosity of nanofluids decreases by increasing temperature. The data on temperature dependence of viscosity of nanofluids were fitted VTF equation very well.

Effect of particles size. There are few studies done on the particle size effect on the viscosity of a nanofluid. Maintaining a constant mass of particles in a suspension while reducing the particle size of the solid particles leads to an increase in the number of particles in the system. A higher number of smaller particles results in more particle-particle interactions and an increased resistance to flow and therefore viscosity increases. Pastoriza-Gallego *et al.* [174] investigated the viscosity of CuO in water for different particle sizes and volume concentrations. They used two different samples of CuO with diameter of 23-37 nm and other 11 nm. They measured the viscosity of both samples and realized that the sample containing smaller size exhibits larger viscosity.

Effect of particle size distribution. Nanofluids which have a wide particle distribution tend to pack better than those of narrow particle distribution keeping constant volume fraction (Fig. 1). This basically means that a wide distribution of particles has more free space to move around which therefore means it is easier for the sample to flow, *i.e.* a lower viscosity.

Effect of shear rate. According to the behavior of nanofluids with respect to the variation in shear rate, they can be divided to Newtonian and non-Newtonian fluids. Newtonian fluids have the following features:

1. Their viscosity is dependent only on temperature but not on shear rate and time.
2. The shear rate is proportional to the shearing stress.
3. The ratio of the shear stress to shear rate is a constant which is called viscosity.

In contrast, a non-Newtonian fluid does not obey the above properties. There are several types of non-Newtonian flow behavior, characterized by the way a fluid's viscosity changes in response to variations in shear rate. Figure 2 shows the most common types of non-Newtonian fluids. Usually, as shear rate increases, particle-particle interactions become relatively weak and even broken down and hence a nanofluid shows the Newtonian behavior.

Namburu *et al.* [168] showed that the nanofluids of CuO nanoparticles in ethylene glycol and water exhibit Newtonian

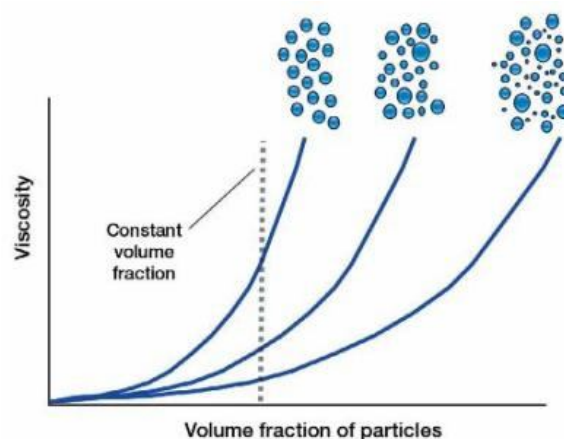


Fig. 1. Viscosity versus volume fraction for nanofluids with different particle size distributions.

flow behavior at low nanoparticle concentrations. In contrast, the nanofluids of cobalt nanoparticles in ethylene glycol and water exhibit non-Newtonian flow behavior.

Abareishi *et al.* [175] measured the rheological properties of nanofluids of α -Fe₂O₃ nanoparticles in glycerol. They found that although glycerol show Newtonian behavior, the nanofluids are non-Newtonian fluids with shear-thinning behavior.

Effect of surfactant. The concentration of the surfactant affects the viscosity of nanofluids. Li *et al.* [176] measured the transport properties of Fe₃O₄/water magnetic nanofluids. They investigated the effect of the surfactant concentrations on the viscosity and indicated that the viscosity of the nanofluids increases with increasing the concentration of the surfactant.

Effect of particle volume concentration. Numerous investigations have been carried out to show the effect of particle concentration on rheological properties for various nanofluids. Almost all of these studies showed that viscosity of a nanofluid is higher than that of its base fluid and increases with an increase in the nanoparticle concentration. As the particle volume fraction increases, the number of particles increases and hence viscosity increases.

Fedele *et al.* [177] measured the viscosity of water-based nanofluids containing titanium oxide as a function of nanoparticle composition. Their results showed that the deviations of nanofluid and water viscosities are about 20%, 60%, and 215% at 10 wt%, 20 wt%, and 35 wt% of TiO₂

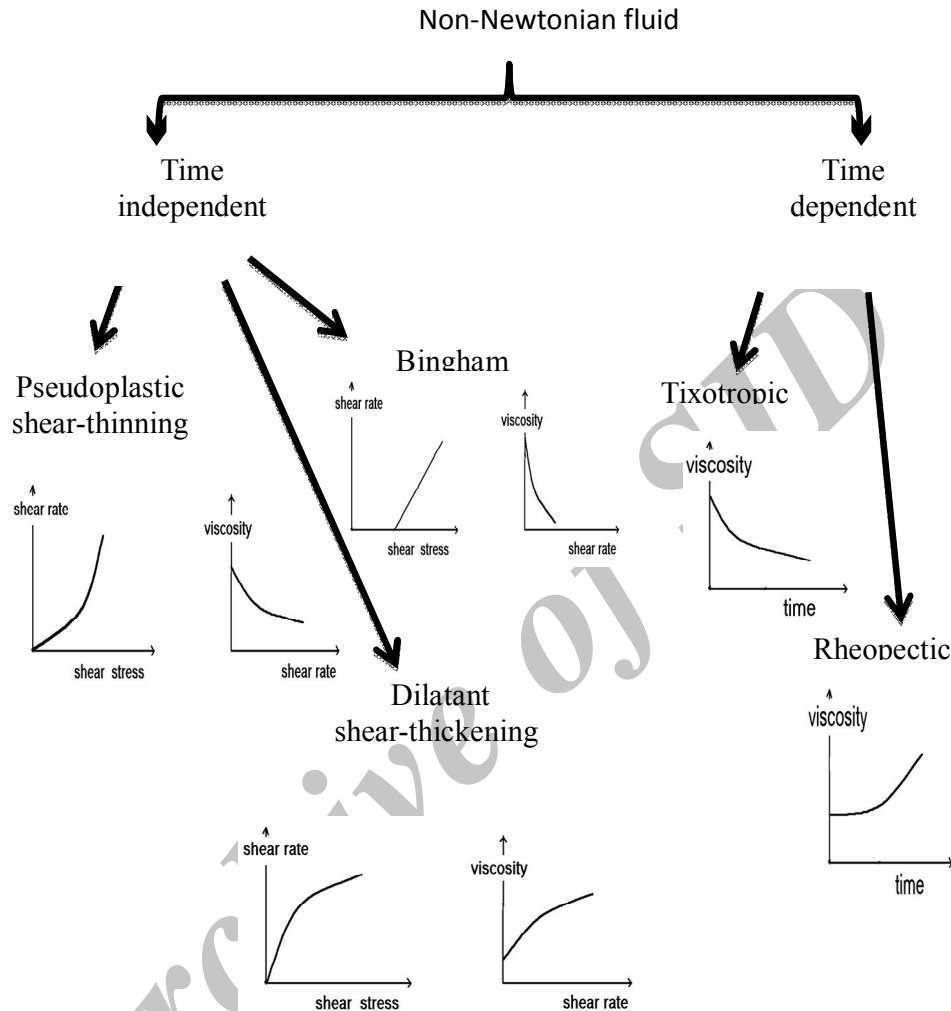


Fig. 2. The most common types of non-Newtonian fluids.

concentration, respectively. The enhancement of viscosity by increasing nanoparticle concentration is not always consistent. For instance, Hojjat *et al.* [178] measured the rheological behavior of suspensions of γ - Al_2O_3 , TiO_2 , and CuO nanoparticles in an aqueous solution of carboxymethyl cellulose at different temperatures. They found that the viscosity of nanofluids and those of the base fluid is a function of temperature and particle concentration. They observed that the relative apparent viscosity of Al_2O_3 and TiO_2 nanofluids increase with increasing nanoparticle concentration but the viscosity of CuO nanofluids is almost independent of nanoparticle concentration.

Some models for predicting viscosity of nanofluids. The effective dynamic viscosity of nanofluids, η , can be calculated using different formulas for two-phase mixtures [179]. A summary of some models for viscosity of nanofluids are listed in Table 4.

Density

By assuming that nanoparticles are well dispersed in the base-fluid, the effective physical properties like density of nanofluids were studied as two-phase fluids using some classical formulas [191,192].

The density of a nanofluid, ρ , is the weighted average of

Table 4. Some Models for Predicting the Viscosity of Nanofluids

Entry	Model	Correlation	Remarks	Ref.
1	Einstein (1906)	$\eta = \eta_f (1 + 2.5\varphi)$	Spherical particles and low particle volume fractions, $\varphi < 0.02$ are considered	[165]
2	Brinkman (1952)	$\eta = \eta_f \frac{1}{1 - \varphi}^{2.5}$	Extended Einstein formula and for concentration lower than 4%	[180]
3	Frankel and Acrivos (1967)	$\eta = \eta_f \frac{9}{8} \left[\frac{(\frac{\varphi}{\varphi_m})^{\frac{1}{5}}}{1 - (\frac{\varphi}{\varphi_m})^{\frac{1}{5}}} \right]$	φ_m must be determined experimentally	[181]
4	Lundgren (1972)	$\eta = \eta_f (1 + 2.5\varphi + 6.25\varphi^2 + o(\varphi^3))$	Taylor series for φ	[182]
5	Batchelor (1977)	$\eta = \eta_f (1 + 2.5\varphi + 6.5\varphi^2)$	Brownian motion is considered	[183]
6	Graham (1981)	$\eta = \eta_f (1 + 2.5\varphi + \frac{4.5}{(\frac{h}{d_p})(2 + \frac{l}{d_p})(1 + \frac{l}{d_p})^2})$	Considering the effect of the minimum separation distance between two spheres is	[184]
7	Tseng and Chen(2003)	$\eta = \eta_f \times 0.4513e^{0.6965\varphi}$	Unrealistic after solids loading ~ 0.07	[185]
8	Cheng and Law (2003)	$\eta = 1 + 2.5\varphi + (2.5\varphi)^2 + (2.5\varphi)^3 + (2.5\varphi)^4 + (2.5\varphi)^5 + \dots$	For two-phase flow with particles larger than 100 nm	[186]

Table 4. Continued

9	Toda and Furuse (2006)	$\eta = \frac{1 + 0.5k\phi - \phi}{(1 - k\phi)^2(1 - \phi)}$	For the concentrated dispersion of large particles	[187]
10	Nguyen <i>et al.</i> (2007)	$\eta = \eta_f(1.1250 - 0.0007T)$	For calculating viscosity of nanofluids at particle concentrations of 1% and 4%	[188]
11	Chen <i>et al.</i> (2007)	$\eta = \eta_f \left(1 - \frac{\phi}{\phi_m} \left(\frac{d_a}{d}\right)^{1.2}\right)^{-[\eta]\phi_m}$	Considering aggregates	[169]
12	Namburu (2007)	$\log \eta = Ae^{-BT}$	A = 1.8375(φ) ² - 29.643(φ)+165.56 B = 4 × 10 ⁻⁶ (φ) ² - 0.001 (φ)+0.0186	[168]
13	Masoumi (2009)	$\eta = \eta_f + \frac{\rho_p V_B d^2}{72Cl}$	Considering the influence of temperature, nanoparticle density, and the base fluid physical properties	[189]
14	Yang (2012)	$\eta = \eta_f \left(1 + 2.5 \left(\frac{d_p + t + h}{d_p}\right)^3 \phi\right)$	Considering the salvation effect	[190]

η : viscosity of nanofluid; η_f : viscosity of base fluid; ϕ_m : maximum particle fraction; d : diameter of nanoparticles; d_p : particle radius, l : interparticle spacing; ρ_p : density of nanoparticles; V_B : Brownian velocity; C : correction factor; t : thickness of the monolayer adsorption layer; h : thickness of the salvation shell.

the base fluid and nanoparticle densities is calculated according to Pak and Cho's [193] equation:

$$\rho = (1 - \phi)\rho_f + \phi\rho_p \quad (20)$$

where ρ_f and ρ_p are the densities of base fluid and nanoparticles, respectively. As this equation shows the density of a nanofluid is a linear function of volume fraction. For typical nanofluids with nanoparticles at less than 1% volume fraction, a change of less than 5% in the fluid density is expected [138].

Specific Heat

Pak and Cho [193] proposed the following equation for specific heat of a nanofluid:

$$C_p = (1 - \phi)C_{pf} + \phi C_{pn} \quad (21)$$

where C_{pf} and C_{pn} are the specific heats of a base fluid and nanoparticles, respectively.

Xuan and Roetzel [194] suggested the other equation:

$$\rho C_p = (1 - \phi)\rho_f C_{pf} + \phi \rho_n C_{pn} \quad (22)$$

Using Eq. (22), one can predict that small decrease in specific heat typically results when solid particles are dispersed in liquids. For example, adding 3 vol% Al₂O₃ to water would be predicted to decrease the specific heat by approximately 8% compared with that of water alone [138].

Due to the lack of specific heat data for the particular nanofluid under study, both expressions are considered equivalent and either one can be used to calculate the specific heat.

The above simple equations may need to be modified if nanoparticles are found to exhibit a size-dependent specific

heat [138].

Surface Tension

Although the heat-transfer properties of nanofluids have been extensively reported in the literature, little is known regarding the surface tension of nanofluids.

Moosavi *et al.* [71] measured the surface tension of ZnO nanoparticles in the ethylene glycol and glycerol. Ammonium citrate as a dispersant was used to improve the stability of nanofluids. They showed that surface tension of suspensions increases with increasing the volume fraction of the solid nanoparticles.

Chen *et al.* [195] measured the surface tension of three nanofluids using the pendant droplet method. The nanoparticles were laponite, silver, and Fe₂O₃. De-ionized water as the base fluid. They found that the Stefan equation related to the apparent surface tension is not suitable for the nanofluids.

The surface tension of ethanol and n-decane based nanofluid fuels containing suspended aluminum, aluminum oxide, and boron nanoparticles as well as dispersible multi-wall carbon nanotubes were measured using the pendant drop method [196]. The effects of nanoparticle concentration, size, and the presence of a dispersing agent (surfactant) on surface tension were determined. They showed that surface tension increases both with particle concentration (above a critical concentration) and particle size for all cases. This is because the van der Waals force between particles at the liquid/gas interface increases surface free energy and thus increases surface tension. At low particle concentrations, addition of particles has little influence on surface tension because of the large distance between particles.

THEORETICAL STUDIES ON NANOFLUIDS

Conduction-based models cannot correctly predict the thermal conductivity of the nanofluids. Therefore, it is important to prepare “computational models” to gain a better fundamental understanding about the thermal properties of nanofluids [148].

Usually, a theoretical approach on the thermal conductivity enhancement in nanofluids is based on mathematical simulations. It is of interest to consider how such

mathematical tools can assist basic science in understanding this phenomenon [197].

Computational approaches to heat transfer problems span from numerical solutions of Fourier’s law to calculations based on the Boltzmann transport equation (BTE) to atomic-level simulations. In the Fourier and BTE approaches, the physics of heat transfer and phonon scattering are incorporated into the calculations in an explicit manner; thus for a reliable calculation, an understanding of the fundamental phonon processes is required. Molecular dynamics (MD) simulation, by contrast, merely involves the integration in time of Newton’s equations of motion for an ensemble of atoms interacting with each other through an, usually empirical, interatomic potential. Because the formalism of the MD approach does not require any a priori understanding of heat transport, it is ideal for investigating the fundamental heat-transfer mechanisms. However, MD does have the significant limitation of being entirely classical, with each vibrational mode equally excited; thus it is only rigorously applicable to solids above the Debye temperature [198].

The thermal conductivity can be computed either using non-equilibrium MD (NEMD) or equilibrium MD. The two most commonly used approaches to the MD simulation of the thermal conductivity are the Green-Kubo method [199] in which the equilibrium fluctuations in the heat current are analyzed, and the “direct method,” which mimics experiment by imposing a temperature gradient on the system and determining the thermal conductivity from Fourier’s law [200]. While simple in principle, in practice each has significant complications associated with system-size effects and requires relatively long simulation times.

Bhattacharya *et al.* [148] developed a technique to compute the effective thermal conductivity of a nanofluid using Brownian dynamics simulation which had the advantage of being computationally less expensive than MD and coupled with the equilibrium Green-Kubo method. Comparing the results with the available experimental data showed that their technique predicts the thermal conductivity of nanofluids to a good level of accuracy.

Xue *et al.* [201] used NEMD simulations to investigate the effect of the layered liquid on the enhancement of the thermal conductivity. They found that for a monatomic base fluid, there is almost no effect on the thermal transport property of

the suspension.

An interesting simulation attempt was published by Shenogin *et al.* [202]. They employed classical MD to study the interfacial resistance for heat flow between a CNT and octane liquid. They found that the interfacial resistance has a large value due to the weak coupling of the nanotube and the liquid which reduced as the length of the nanotube increases.

By considering the external and internal forces acting on suspended nanoparticles as well as mechanical and thermal interactions among nanoparticles and fluid particles, a thermal lattice Boltzmann model was proposed by Xuan *et al.* [203] for simulating flow and energy transport process of the nanofluid. They carried out some numerical computations by considering a nanofluid flowing through a channel as an example and discussing on the mechanism of enhancement of heat transfer.

Vladkov and Barrat [204] used the MD simulations to simulate the thermal properties of a model fluid containing nanoparticles. By modelling transient absorption experiments, they showed a reliable determination of interfacial resistance between the particles and the fluid. The flexibility of molecular simulation allowed them to consider separately the effect of confinement, particle mass, and Brownian motion on the thermal transfer between fluid and particles. They showed that in the absence of collective effects, the heat conductivity of the nanofluid is well described by the classical Maxwell Garnet model.

Prasher *et al.* [205] presented a three-level homogenization theory to evaluate the effective thermal conductivity of colloids containing fractal clusters. In particular, their treatment allowed the estimation of the effect of cluster morphology in terms of the average radius of gyration, R_g , of the aggregates and the fractal and chemical dimensions of the aggregates (d_f and d_i , respectively). They demonstrated that such fractal aggregates lead to thermal conductivity enhancement that can be significantly higher than that of predicted values using homogenization theories of well-dispersed composites. The authors validated the presented homogenization model by comparison with Monte Carlo (MC) numerical calculations of thermal conductivity of structures obtained by diffusion limited cluster-cluster aggregation algorithms.

Eapen *et al.* [206] quantitatively assessed the thermal conduction modes in a nanofluid by combining linear response theory with MD simulations. Their findings revealed a molecular-level mechanism for enhanced thermal conductivity in nanofluids with short-ranged attraction. In another work, Eapen *et al.* [207] using NEMD, demonstrated that the thermal conductivity of a well-dispersed nanofluid was enhanced beyond the Maxwell limit through a percolating amorphous-like fluid structure at the cluster interface. They showed that these interconnected paths emerged only when the cluster-fluid interaction was strong. The attendant changes in interfacial structure were accessible by experimental techniques such as neutron scattering.

Sarkar *et al.* [208] used an equilibrium MD simulation to compute the thermal conductivity of the base fluid and nanofluid using the Green-Kubo method for various volume fractions of nanoparticle. Their study showed the ability of MD to predict the enhanced thermal conductivity of nanofluids. They investigated the mechanisms involved in thermal transport of nanofluids at the atomic level. Their computations showed that the thermal transport enhancement of nanofluids was mostly due to the increased movement of liquid molecules in the presence of nanoparticle.

Li *et al.* [209] investigated the molecular layering at liquid-solid interface in a nanofluid by equilibrium MD simulation. The shape of the nanoparticles was spherical and the volume fraction was 1.5% for nanoparticles with diameter of 1.75 nm in the computational domain. By tracking the positions of the nanoparticles and the liquid atoms, they found that an adsorbed slip layer of liquid is formed at the interface between the nanoparticles and liquid; this thin layer will move with the Brownian motion of the nanoparticles.

Vladkov *et al.* [210] used MD simulation to compute the thermal properties of a nanofluid. The flexibility of molecular simulation allowed them to consider the effects of particle mass, particle-particle and particle-fluid interaction, and the spatial distribution of the particles on the thermal conductivity. They showed that the heat conductivity of a well dispersed nanofluid is well described by the classical Maxwell-Garnet equation model.

Sankar *et al.* [211] proposed a theoretical approach based on MD modeling for the estimation of the enhancement of the thermal conductivity of liquids by the introduction of

suspended metallic nanoparticles. The thermal conductivity enhancement estimated using the simulations are compared with existing experimental results and those predicted by conventional effective medium theories.

Lu *et al.* [212] used a stationary nanofluids of the volume fractions less than 8% and a simplified MD simulation method to simulate the thermophysical properties of nanofluids. Authors presented a good agreement between numerical results and experimental data. They also showed that the simplified dynamics simulation method was an effective method to forecast some thermal properties of nanofluids. They studied the effects of the volume fraction and the size of nanoparticles on the thermal conductivity and the viscosity of nanofluids. Numerical results showed that decreasing size of nanoparticles or increasing the volume fraction can increase thermal conductivity with increasing viscosity.

Mohebbi [213] used a new method based on combination of equilibrium and non-equilibrium MD simulation in a non-periodic boundary conditions to calculate the thermal conductivity. In this method, first the specific heat and the thermal diffusivity of a nanofluid were determined by equilibrium MD and NEMD. Then, the thermal conductivity was calculated from the relation of thermal diffusivity with the constant volume specific heat. This approach was tested by the nanofluid of silicon nitride nanoparticles in liquid argon. They compared the results of simulation for the base fluid at different temperatures with experimental data. The effects of temperature and nanoparticle loadings on the thermal conductivity were investigated by the authors. Their results showed that thermal conductivity increases with increasing the loadings and decreasing the temperature.

Kang *et al.* [214] studied non-equilibrium heat transfer in a copper/argon nanofluid by MD simulation. They introduced two different methods, the physical definition method and the curve fitting method, to calculate the coupling factor between nanoparticles and base fluid. Their results showed that the coupling factors obtained by these two methods are consistent. The coupling factor was proportional to the volume fraction of the nanoparticles and inversely proportional to nanoparticle diameter. They showed that in the temperature range of 90-200 K, the coupling factor is not affected by temperature. The nanoparticle aggregation led to a decrease of the coupling factor.

Seyf *et al.* [215] presented numerical investigation on the application of nanofluids in Micro-Pin-Fin heat sinks (MPFHSS). To investigate the flow and heat transfer behavior in MPFHSSs, three-dimensional steady Naviere-Stokes and energy equations were solved iteratively. The nanofluids were CuO/deionized water (the mean diameters of nanoparticles are 28.6 and 29 nm) and Al₂O₃/deionized water (the mean diameters of nanoparticles were 38.4 and 47 nm). The results showed that (i) a significant enhancement of heat transfer occurs in the MPFHSS due to suspension of CuO or Al₂O₃ nanoparticles in the base fluid in comparison with pure water, (ii) enhancement of heat transfer is intensified with increasing volume fraction of nanoparticles and Reynolds number, (iii) increasing volume fraction of nanoparticles which is responsible for higher heat transfer performance leads to higher pressure drop, (iv) with decreasing particle diameters the Nusselt number increases for Al₂O₃/water nanofluid while the trend was reverse for CuO/water nanofluid.

Dang *et al.* [216] carried out MD simulations to systematically study solvation and particle-particle interactions in n-hexane, water, and methanol fluids. Their results indicated that dynamics of n-hexane molecules was significantly influenced by solvated nanoparticles. Water and methanol showed significant structural signatures binding to the metal coordination sites of the nanoparticles while liquid hexane did not.

Lin *et al.* [217] calculated the thermal conductivity and revealed molecular-level mechanisms for copper nanoparticles suspended in ethylene glycol using MD simulations. Computed thermal conductivities of the nanofluids using Green-Kubo formalism and using non-equilibrium MD methods were compared. The simulations confirmed that the enhancement of thermal conductivity due to the suspending nanoparticle increased with volume fraction and the size of the nanoparticles.

Gao *et al.* [218] used MD simulations to study the interaction of functionalized CNTs (FCNT) with an immersed metal surface and the effects of the interaction on the thermal properties of the FCNT nanofluid and the heat transfer during rapid heating. They discussed the thermal properties of the nanofluid and the heat transfer characteristics with the atomistic details of the interactions of the FCNT with the solid surface and the water molecules. The results of the

simulation provided a new thermal transport mechanism which could be able to explain and predict the enhancement of the heat transfer of nanofluids more accurately.

However, there have been no conclusive computational results shown so far, probably because of the huge computational costs associated with the MD method.

APPLICATIONS OF NANOFUIDS

The application of nanofluids is so diverse that need several separate review articles. Here, we will focus on some important non-biological and biological applications.

Non-biological Applications

Tsai *et al.* [219] employed an aqueous nanofluid of various sizes of gold nanoparticles as working medium for conventional circular heat pipe. The heat pipe was designed as a heat spreader for a notebook CPU or a desktop PC. They observed a significant reduction in thermal resistance of heat pipe with nanofluid compared with deionized water.

Tzeng *et al.* [220] studied the use of nanofluids as engine coolants. To make the experimental conditions match the real operation as close as possible, the real RBC of a power transmission system of a real-time four-wheel-drive (4WD) vehicle was adopted. They mixed CuO (4.4% wt) and Al₂O₃ (4.4% wt) nanoparticles and antifoam individually with automatic transmission oil. The experimental platform was a 4WD transmission system. The experimental results showed that, under similar conditions, antifoam-oil provides the highest temperature distribution in rotary blade coupling and, accordingly, the worst heat transfer effect was obtained. CuO/oil provides the lowest temperature distribution both at high and low rotating speed and, accordingly, the best heat transfer effect was observed.

Nguyen *et al.* [221] investigated the heat transfer enhancement and behavior of the nanofluid of Al₂O₃ nanoparticles in distilled water for use in a closed cooling system destined for microprocessors or other heated electronic components. They showed that the inclusion of nanoparticles into distilled water produces a considerable enhancement of the cooling convective heat transfer coefficient. For a particular particle volume concentration of 6.8%, the heat transfer coefficient was found to increase as

much as 40% compared to that of the base fluid.

Park *et al.* [222] investigated the effect of CNTs on the boiling of two halocarbon refrigerants for building air-conditioning applications. To investigate the heat transfer enhancement with CNTs, two halocarbon refrigerants (R123 and R134a for building chillers) were used as working fluids and 1.0 vol.% of CNTs was added to the working fluids. The results indicated that CNTs increase nucleate boiling heat transfer coefficients for these refrigerants up to 36.6%.

Choi *et al.* [223] prepared some kinds of nanofluids by dispersing Al₂O₃ and AlN nanoparticles in transformer oil. They showed that AlN nanoparticles at a volume fraction of 0.5% can increase the thermal conductivity of the transformer oil by 8% and the overall heat transfer coefficient by 20%. From the natural convection test using a prototype transformer, the cooling effect of Al₂O₃/AlN-oil nanofluids on the heating element and oil itself was confirmed by the authors. They showed that these nanofluids have the potential of being recognized as a new generation of coolants for vehicle thermal management due to their significantly higher thermal conductivities than the base fluids.

Leong *et al.* [224] studied the application of ethylene glycol based copper nanofluids in an automotive cooling system. They observed that overall heat transfer coefficient and heat transfer rate in engine cooling system increase with the usage of nanofluids compared to ethylene glycol alone. They showed that about 3.8% of heat transfer enhancement could be achieved with the addition of 2% copper particles in a base fluid at the Reynolds number of 6000 and 5000 for air and coolant, respectively.

Phelan *et al.* [225] used different nanoparticles (CNTs, graphite, and silver) to prepare nanofluids and investigated the efficiency of solar collectors based on nanofluids. They demonstrated up to 5% efficiency improvements in solar thermal collectors by utilizing nanofluids.

Firouzfard *et al.* [226] used the silver/methanol nanofluid filled thermosyphon heat exchanger and investigated the effectiveness and energy saving of the system. Their experimental results indicated that using silver/methanol nanofluid instead of pure methanol, leads to energy saving around 8.8-31.5% for cooling and 18-100% for reheating the supply air stream in an air conditioning system.

Nanofluids can be applied in grinding as effective cooling

and lubrication to control the grinding temperature. Vasu and Kumar [227] developed a new cutting fluid, TRIM E709 emulsifier with Al_2O_3 nanoparticles, in order to avoid thermal damage at the grinding zone. They showed that using TRIM E709 emulsifier with Al_2O_3 nanoparticles, reduce the temperatures from 20% to 30%. They also found that application of TRIM E709 emulsifier with Al_2O_3 nanoparticle decreased the energy partition and surface roughness.

Yousefi *et al.* [228] investigated the effect of Al_2O_3 /water nanofluid on the efficiency of a flat-plate solar collector. The weight fraction of nanoparticles was 0.2% and 0.4% and the particles dimension was 15 nm. Their results indicated that using the nanofluids as a working fluid compared with water as an adsorption medium increase the efficiency. They reported 28.3% enhancement of efficiency by applying 0.2 wt% of nanofluids.

Saidur *et al.* [229] studied the effect of nanofluid in direct solar collector. They investigated the effect of size and volume fraction of nanoparticles on the extinction coefficient of water based aluminium nanofluid. Their results showed that using 1.0% volume fraction of nanofluid leads to the significant improvement in the efficiency of the solar collector.

Ijam *et al.* [230] used nanofluids with different volume fractions as a promising coolant for electronic systems. They used a minichannel heat sink for SiC/water and TiO_2 /water nanofluids as coolants. Their results indicated 12.44% and 9.99% enhancement in thermal conductivity for SiC/water and TiO_2 /water nanofluids for 4% volume fraction, respectively. They found that using SiC/water and TiO_2 /water nanofluids as coolant instead of water leads to an improvement of approximately 7.25%-12.43% and 7.63%-12.77%, respectively.

Moraveji and Razvarz [231] investigated the effect of aluminum oxide (35 nm)/water nanofluids on the thermal efficiency enhancement of a heat pipe on different operating systems. They changed the concentration of nanofluid in the range of 0% to 3% wt. Their results showed that using the nanofluids in the heat pipe increases the thermal performance by reducing the thermal resistance.

Biological Applications

Applications of nanofluids in medicine and biology are

diverse including but not limited to drug encapsulation and precise delivery to inaccessible tissues deep inside the body called nanodrug delivery. For the sake of brevity, we will focus on the biological applications of heat transfer enhancement of nanofluids. Because the biological applications of nanofluids are not the main goal of this review article, we limit the applications to using nanofluids to improve the performance of technically challenging methods in biology and medicine.

Laser surgery. Pulsed lasers have been used extensively in laser surgery as nanoblades. A tightly focused laser beam is well capable of inducing hot localized plasma for rapid heating to destroy the tumour cells. Hot local spots will indiscriminately ruins healthy and cancerous cells. Efficient and fast heat dissipation is critical to save the healthy cells in close proximity to targeted tumour cells. Creating a nanofluid environment surrounding the tumour cells will efficiently acts as a heat sink to preserve the health tissues while localized laser plasma destroys the tumour cells [232].

A photothermal nanoblade. The photothermal nanoblade is a new approach for delivering difficult cargo into mammalian cells. Controlled cutting of mammalian cell membranes is very difficult and it is a technically challenging task because the cell membranes are elastic, mechanically fragile, and rapidly reseal. A photothermal nanoblade with a metallic nanostructure could harvest short laser pulse energy and convert it into a highly localized explosive vapour bubble. These bubbles puncture rapidly and a lightly contacting cell membrane, *via* high-speed fluidic, flows and induces transient shear stress. The cavitation bubble pattern is controlled by the configuration of metallic structure, laser pulse duration and laser energy. It was reported that integration of the metallic nanostructure with a micropipet, could generate a micrometer-sized nanoblade to access membrane port and deliver 5×10^8 live bacteria/ml with 46% efficiency and more than 90% cell viability into mammalian cells. Additional cargo over 3-orders of magnitude in size including DNA, RNA, 200 nm polystyrene Beads, and 2 μm bacteria have also been delivered into multiple mammalian cell types [232].

Nanocryosurgery. Cryosurgery uses freezing to destroy undesired tissues. Loading high thermal conductivity nanoparticles into the target tissues reduces the final

temperature, increases the maximum freezing rate and enlarges the ice volume obtained in the absence of nanoparticles. Magnetite Fe_3O_4 and diamond nanofluids have been reported to enhance freezing because of their good biological compatibility. Particle sizes less than $10\ \mu\text{m}$, either *via* encapsulation in a larger moiety or suspension in a carrier fluid, are small enough for effective delivery to the site of the tumour. Introduction of nanoparticles into the target *via* a nanofluid would effectively increase the nucleation rate at a high temperature threshold [233].

Long PCR efficiency enhancement. PCR is the most common method in molecular biology and medicine used mostly for DNA amplification and disease diagnosis. The PCR machines use a Peltier to apply a series of heating and cooling cycles to amplify DNA. The efficiency of the PCR depends strongly on the PCR system's heating/cooling ratio and the rate of temperature changes of the Peltier plates. The other problem is the lack of efficiency in long PCR. No mature technology is available to amplify very long, 100 kb, DNA sequences with GC-rich long DNA fragments. Long DNA amplification is critical for cloning and in functional genomics studies. There are a series of reports on CNT in the context of their interaction with DNA polymerase enzymes and thus increase the activity and stability of the polymerase. It has also been reported that the thermal conductivity of individual MWCNTs is up to $3000\ \text{W m}^{-1}\ \text{K}^{-1}$, and $6000\ \text{W m}^{-1}\ \text{K}^{-1}$ for SWCNTs. The thermal conductivity of the bulk CNTs is lower than that of single CNTs. When CNTs are dispersed in different phases, the measured thermal conductivity of the suspensions shows a remarkable enhancement in comparison with the dispersed phase as the working fluid. These observations suggest that the PCR in the presence of aqueous suspension of CNTs would have a higher thermal conductivity, causing a rapid thermal equilibrium and convection heat transfer. Therefore, the temperature of the PCR system in the presence of nanofluids would be more uniform, and the time delay between the thermal block temperature and the sample temperature is also likely to decrease. PCR efficiency increases significantly when the specific annealing of primers with templates, and the chance of nonspecific or smear products formation is decreased. An aqueous suspension of CNTs results improvement of long PCR specificity. Both SWCNTs and MWCNTs significantly

enhance the specificity of long PCR. The possible mechanisms could include the enhancement of heat equilibrium and the interaction of CNTs directly with reaction components. Different types of nanoparticles have been reported for their beneficial effects on PCR: Au, Ag, carbon nanopowder, CNT, Pt, and nano-alloys. The collective observations of the literatures suggest that nanofluid could be a novel platform to develop a new generation of recombinant DNA technologies [234].

CONCLUDING REMARKS AND FUTURE CHALLENGES

The present review provides a comprehensive outline of the attractive research progress made in the area of nanofluids with the emphasis on heat transfer enhancement. Considerable research and development focusing on nanofluids have been carried out. This review summarized the developments in experiment, theory, and computation in the field.

Even though the available data provide interesting insight into nanofluid properties and heat transfer benefits, a considerable amount of research remains to be done on this fascinating subject and the development of the field faces several challenges. We conclude by outlining several important issues that we believe nanofluids should receive greater attention in the future:

1. To improve existing synthesis techniques or to develop new nanoparticle synthesis and dispersion techniques that will enable systematic study of a series of nanofluids.
2. To develop processing techniques that will allow synthesis of larger quantities of nanofluids with non-agglomerated nanoparticles.
3. The experimental data on physical properties of nanofluids especially thermal conductivity are very scattered. Even though data provide insight into nanofluid properties and heat transfer benefits, a considerable amount of research remains to be done on this subject.
4. The size distribution of nanoparticles and nanoparticle aggregates in the suspensions are rarely reported. This lack of data can be attributed to the difficulty in properly characterizing high-concentration suspensions of nanoparticles, *e.g.* light scattering techniques work poorly or not at all at high particle concentrations. Cryogenic

transmission electron microscopy might provide a powerful characterization method but few materials laboratories are equipped to apply this technique [235].

5. More study on the effects of particle surface treatment on thermal behavior is needed.

6. More application-oriented researches are required on nanofluids and it is expected to grow at a faster rate in the future.

7. Although, the number of models for prediction of thermal conductivity of nanofluids is very high, the mechanism of thermal conductivity enhancement is still unclear. It requires further computational studies to understand all of the factors that affect on this enhancement.

REFERENCES

- [1] S.U.S. Choi, in: D.A. Singer, H.P. Wang (Eds.), *Enhancing Thermal Conductivity of Fluids with Nanoparticles*, Developments and Applications of Non-newtonian Flows, American Society of Mechanical Engineers, New York, 1995.
- [2] S. Lee, S.U.S. Choi, S. Li, J.A. Eastman, *J. Heat Transf.* 121 (1999) 280.
- [3] S.K. Das, N. Putra, W. Roetzel, *Int. J. Heat Mass Tran.* 46 (2003) 851.
- [4] K.S. Kim, M.H. Won, J.W. Kim, B.J. Back, *Appl. Therm. Eng.* 23 (2003) 1137.
- [5] J.C. Maxwell, *A Treatise on Electricity and Magnetism*, Oxford University Press, Cambridge, 1904.
- [6] G.K. Batchelor, *J. Fluid Mech.* 83 (1977) 97.
- [7] S.K. Gupte, S.G. Advani, P. Huq, *Int. J. Heat Mass Tran.* 38 (1995) 2945.
- [8] H. Masuda, A. Ebata, K. Teramae, N. Hishinuma, *Netsu Bussei* 4 (1993) 227.
- [9] J.A. Eastman, S.U.S. Choi, S. Li, L.J. Thompson, S. Lee, *Materials Research Society Symposium Proceedings*, 1996.
- [10] X. Wang, X. Xu, S.U.S. Choi, *J. Thermophys. Heat Tr.* 13 (1999) 474.
- [11] P. Keblinski, J.A. Eastman, D.G. Cahill, *Mater. Today* 8 (2005) 36.
- [12] Y. Xuan, Q. Li, *Int. J. Heat and Fluid Flow* 21 (2000) 58.
- [13] H. Chang, T.T. Tsung, L.C. Chen, C.S. Jwo, J.W. Tsung, Y.C. Lu, *J. Mater. Eng. Perform.* 14 (2005) 158.
- [14] H.U. Kang, S.H. Kim, J.M. Oh, *Exp. Heat Transf.* 19 (2006) 181.
- [15] H.E. Patel, S.K. Das, T. Sundararajan, N.A. Sreekumaran, B. George, T. Pradeep, *Appl. Phys. Lett.* 83 (2003) 2931.
- [16] H. Boennemann, S.S. Botha, B. Bladergroen, V.M. Linkov, *Appl. Organomet. Chem.* 19 (2005) 768.
- [17] C.H. Lee, S.W. Kang, S.H. Kim, *J. Ind. Eng. Chem.* 11 (2005) 152.
- [18] T. Cho, I. Baek, J. Lee, S. Park, *J. Ind. Eng. Chem.* 11 (2005) 400.
- [19] S.W. Kang, W.C. Wei, H.S. Tsai, S.Y. Yang, *Appl. Therm. Eng.* 26 (2006) 2377.
- [20] C.H. Lo, T.T. Tsung, H.M. Lin, *J. Alloy Compd.* 434-435 (2007) 659.
- [21] S.K. Das, N. Putra, P. Thiesen, W. Roetzel, *J. Heat Transf.* 125 (2003) 567.
- [22] S.M. You, J.H. Kim, K.H. Kim, *Appl. Phys. Lett.* 83 (2003) 3374.
- [23] S.E.B. Maiga, C.T. Nguyen, N. Galanis, G. Roy, *Superlattice Micros.* 35 (2004) 543.
- [24] D. Wen, Y. Ding, *Int. J. Heat Mass Tran.* 47 (2004) 5181.
- [25] S.E.B. Baiga, S.J. Palm, C.T. Nguyen, G. Roy, N. Galanis, *Int. J. Heat and Fluid Flow* 26 (2005) 530.
- [26] J.K. Kim, J.Y. Jung, Y.T. Kang, *Int. J. Refrig.* 29 (2005) 22.
- [27] J.K. Kim, J.Y. Jung, Y.T. Kang, *Int. J. Refrig.* 30 (2006) 50.
- [28] C.T. Nguyen, G. Roy, N. Galanis, S. Suiro, *Tran. on Heat and Mass Transf.* 1 (2006) 370.
- [29] X. Zhang, H. Gu, M. Fujii, *Int. J. Thermophys.* 27 (2006) 569.
- [30] S.J. Palm, G. Roy, C.T. Nguyen, *Appl. Therm. Eng.* 26 (2006) 2209.
- [31] X. Zhang, H. Gu, M. Fujii, *Netsu Bussei* 20 (2006) 14.
- [32] S.Z. Heris, S.G. Etemad, M.N. Esfahany, *Int. Commun. Heat Mass* 33 (2006) 529.
- [33] C.H. Chon, S. Paik, J.B.J. Tipton, K.D. Kihm, *Langmuir* 23 (2007) 2953.

- [34] C.T. Nguyen, G. Roy, C. Gauthier, N. Galanis, *Appl. Therm. Eng.* 27 (2007) 1501.
- [35] S.Z. Heris, M.N. Esfahany, S.G. Etemad, *Int. J. Heat Fluid Flow* 28 (2007) 203.
- [36] D.H. Yoo, K.S. Hong, H.S. Yang, *Thermochim. Acta* 455 (2007) 66.
- [37] S.H. Kim, S.R. Choi, D. Kim, *J. Heat Transf.* 129 (2007) 298.
- [38] C.Y. Tsai, H.T. Chien, P.P. Ding, B. Chan, T.Y. Luh, P.H. Chen, *Mater. Lett.* 58 (2004) 1461.
- [39] X. Zhang, H. Gu, M. Fujii, *J. Appl. Phys.* 100 (2006) 044325.
- [40] M.J. Assael, I.N. Metaxa, K. Kakosimos, D. Constantinou, *Int. J. Thermophys.* 27 (2006) 999.
- [41] D. Milanova, R. Kumar, S. Kuchibhatla, S. Seal, *Proceedings of the Fourth International Conference on Nanochannels, Microchannels and Minichannels, Limerick, Ireland, 2006.*
- [42] J.A. Eastman, S.U.S. Choi, S. Li, W. Yu, L.J. Thompson, *Appl. Phys. Lett.* 78 (2001) 718.
- [43] H.T. Zhu, Y.S. Lin, Y.S. Yin, *J. Colloid Interf. Sci.* 277 (2004) 100.
- [44] D.W. Zhou, *Int. J. Heat Mass Tran.* 47 (2004) 3109.
- [45] R. Chein, G. Huang, *Appl. Therm. Eng.* 25 (2005) 3104.
- [46] C.H. Lo, T.T. Tsung, L.C. Chen, *J. Cryst. Growth* 277 (2005) 636.
- [47] S.P. Jang, S.U.S. Choi, *Appl. Therm. Eng.* 26 (2006) 2457.
- [48] M.S. Liu, M.C.C. Lin, C.Y. Tsai, C.C. Wang, *Int. J. Heat Mass Tran.* 49 (2006) 3028.
- [49] H. Chang, T.T. Tsung, C.R. Lin, H.M. Lin, C.K. Lin, C.H. Lo, H.T. Su, *Mater. Trans.* 45 (2004) 1375.
- [50] C.H. Lo, T.T. Tsung, *Rev. Adv. Mater. Sci.* 10 (2005) 64.
- [51] C.H. Lo, T.T. Tsung, L.C. Chen, C.H. Su, H.M. Lin, *J. Nanopart. Res.* 7 (2005) 313.
- [52] H. Chang, C.S. Jwo, C.H. Lo, T.T. Tsung, M.J. Kao, H.M. Lin, *Rev. Adv. Mater. Sci.* 10 (2005) 128.
- [53] M.S. Liu, C.C. Lin, Y.T. Huang, C.C. Wang, *Nengyuan Jikan* 120 (2005) 120.
- [54] D.P. Kulkarni, D.K. Das, G.A. Chukwu, *J. Nanosci. Nanotechnol.* 6 (2006) 1150.
- [55] H.T. Zhu, C.Y. Zhang, Y.M. Tang, J.X. Wang, *J. Phys. Chem. C* 111 (2007) 1646.
- [56] Z.H. Liu, Y.H. Qiu, *Heat Mass Transf.* 43 (2007) 699.
- [57] Y. Hwang, J.K. Lee, C.H. Lee, Y.M. Jung, S.I. Cheong, C.G. Lee, B.C. Ku, S.P. Jang, *Thermochim. Acta* 455 (2007) 70.
- [58] T.K. Hong, H.S. Yang, *J. Korean Phys. Soc.* 47 (2005) S321.
- [59] T.K. Hong, H.S. Yang, C.J. Choi, *J. Appl. Phys.* 97 (2005) 064311.
- [60] K.S. Hong, T.K. Hong, H.S. Yang, *Appl. Phys. Lett.* 88 (2006) 031901.
- [61] M. Abareshi, S.H. Sajjadi, S.M. Zebarjad, E.K. Goharshadi, *J. Mol. Liq.* 163 (2011) 27.
- [62] C.H. Lo, T.T. Tsung, L.C. Chen, *JSME Int. J. Series B: Fluids and Thermal Eng.* 48 (2005) 750.
- [63] H. Zhu, C. Zhang, S. Liu, Y. Tang, Y. Yin, *Appl. Phys. Lett.* 89 (2006) 023123.
- [64] M. Abareshi, E.K. Goharshadi, S.M. Zebarjad, H. Khandan Fadafan, A. Youssefi, *J. Magn. Magn. Mater.* 322 (2010) 3895.
- [65] S.M.S. Murshed, K.C. Leong, C. Yang, *Int. J. Therm. Sci.* 44 (2005) 367.
- [66] H. Chang, C.S. Jwo, C.H. Lo, C. Su, T.T. Tsung, L.C. Chen, H.M. Lin, M.J. Kao, *Mater. Sci. Technol.* 21 (2005) 671.
- [67] D. Wen, Y. Ding, R.A. Williams, *J. Enhanc. Heat Transf.* 13 (2006) 231.
- [68] S.M.S. Murshed, K.C. Leong, C. Yang, *J. Phys. D: Appl. Phys.* 39 (2006) 5316.
- [69] Y. He, Y. Jin, H. Chen, Y. Ding, D. Cang, H. Lu, *Int. J. Heat Mass Tran.* 50 (2007) 2272.
- [70] A. Ceylan, K. Jastrzembski, S.I. Shah, *Metall. Mater. Trans. A* 37A (2006) 2033.
- [71] M. Moosavi, E.K. Goharshadi, A. Youssefi, *Int. J. Heat and Fluid Flow* 31 (2010) 599.
- [72] M. Chopkar, S. Kumar, D.R. Bhandari, P.K. Das, I. Manna, *Mater. Sci. Eng. B* 139 (2007) 141.
- [73] E.K. Goharshadi, M. Hadadian, *Ceram. Int.* 38 (2012) 1771.
- [74] S.U.S. Choi, Z.G. Zhang, W. Yu, F.E. Lockwood, E.A. Grulke, *Appl. Phys. Lett.* 79 (2001) 2252.
- [75] H.Q. Xie, J.C. Wang, T.G. Xi, Y. Liu, F. Ai, *J. Mater. Sci. Lett.* 21 (2002) 1469.

- [76] H. Xie, H. Lee, W. Youn, M. Choi, *J. Appl. Phys.* 94 (2003) 4967.
- [77] D. Wen, Y. Ding, *J. Thermophys. Heat Tr.* 18 (2004) 481.
- [78] M.S. Liu, M.C.C. Lin, I.T. Huang, C.C. Wang, *Int. Commun. Heat Mass* 32 (2005) 1202.
- [79] Y. Yang, E.A. Grulke, Z.G. Zhang, G. Wu, *J. Nanosci. Nanotechno.* 5 (2005) 571.
- [80] Y. Ding, H. Alias, D. Wen, R.A. Williams, *Int. J. Heat Mass Tran.* 49 (2006) 240.
- [81] H.S. Xue, J.R. Fan, Y.C. Hu, R.H. Hong, K.F. Cen, *J. Appl. Phys.* 100 (2006) 104909.
- [82] S. Das, S.U.S. Choi, H.E. Patel, *Heat Transf. Eng.* 27 (2006) 3.
- [83] M. Yeganeh, N. Shahtahmassebi, A. Kompany, E.K. Goharshadi, A. Youssefi, L. Siller, *Int. J. Heat Mass Tran.* 53 (2010) 3186.
- [84] T.T. Baby, S. Ramaprabhu, *J. Appl. Phys.* 108 (2010) 124308.
- [85] L. Chen, H. Xie, *Thermochim. Acta* 497 (2010) 67.
- [86] E.K. Goharshadi, S. Samiee, P. Nancarrow, *J. Colloid Interf. Sci.* 356 (2011) 473.
- [87] E.K. Goharshadi, M. Abareshi, R. Mehrkhan, S. Samiee, M. Moosavi, A. Yussefi, P. Nancarrow, *Mat. Sci. Semicon. Proc.* 14 (2010) 69.
- [88] E.K. Goharshadi, R. Mehrkhan, P. Nancarrow, *Mat. Sci. Semicon. Proc.* In Press (2012).
- [89] E.K. Goharshadi, S.H. Sajjadi, R. Mehrkhan, P. Nancarrow, *Chem. Eng. J.* 209 (2012) 113.
- [90] M. Abareshi, S.M. Zabarjad, E.K. Goharshadi, *J. Compos. Mater.* 43 (2009) 2821.
- [91] M. Yazdanbakhsh, I. Khosravi, E.K. Goharshadi, A. Youssefi, *J. Hazard. Mater.* 184 (2010) 684.
- [92] I. Khosravi, M. Yazdanbakhsh, E.K. Goharshadi, A. Youssefi, *Mater. Chem. Phys.* 130 (2011) 1156.
- [93] J.A. Eastman, U.S. Choi, S. Li, L.J. Thompson, S. Lee, *Proceedings of the Materials Research Symposium (Nanophase and Nanocomposite Materials II)*, 1997.
- [94] J.A. Eastman, S.U.S. Choi, S. Li, G. Soyez, L.J. Thompson, R.J. DiMelfi, *J. Metastab. Nanocryst.* 2 (1998) 629.
- [95] V.V. Srdic, M. Winterer, A. Moller, G. Miehe, H. Hahn, *J. Am. Ceram. Soc.* 84 (2001) 2771.
- [96] V. Trisaksria, S. Wongwises, *Renew. Sust. Energy Rev.* 11 (2007) 512.
- [97] A. Ghadimi, R. Saidur, H.S.C. Metselaar, *Int. J. Heat Mass Tran.* 54 (2011) 4051.
- [98] H. Xie, J. Wang, T. Xi, Y. Liu, F. Ai, Q. Wu, *J. Appl. Phys.* 91 (2002) 4568.
- [99] D. Lee, J. Kim, B.G. Kim, *J. Phys. Chem. B* 110 (2006) 4323.
- [100] L. Jiang, L. Gao, J. Sun, *J. Colloid Interf. Sci.* 260 (2003) 89.
- [101] X.J. Wang, D.S. Zhu, S.Y. Yang, *Chem. Phys. Lett.* 470 (2009) 107.
- [102] M.J. Assael, I.N. Metaxa, J. Arvanitidis, D. Christofilos, C. Lioutas, *Int. J. Thermophys.* 26 (2005) 647.
- [103] I. Madni, C.Y. Hwang, S.D. Park, Y.H. Choa, H.T. Kim, *Colloids Surface A: Physicochem. Eng. Aspects* 358 (2010) 101.
- [104] H. Zhu, C. Zhang, Y. Tang, J. Wang, B. Ren, Y. Yin, *Carbon* 45 (2007) 226.
- [105] D. Wu, H. Zhu, L. Wang, L. Liua, *Curr. Nanosci.* 5 (2009) 103.
- [106] X.Q. Wang, A.S. Mujumdar, *Int. J. Therm. Sci.* 46 (2007) 1.
- [107] B. Deryagin, L. Landau, *Acta Physicochim.* 14 (1941) 633.
- [108] E.J. Verwey, J.T.G. Overbeek, *Theory of the Stability of Lyophobic Colloids*, Elsevier, New York, 1948.
- [109] B. Olle, S. Bucak, T.C. Holmes, L. Bromberg, T.A. Hatton, D.I.C. Wang, *Ind. Eng. Chem. Res.* 45 (2006) 4355.
- [110] P. Vadasz, *J. Heat Transf.* 128 (2006) 465.
- [111] W. Yu, H. Xie, *J. Nanomater.* (2012) 1.
- [112] D. Wu, H. Zhu, L. Wang, L. Liua, *Curr. Nanosci.* 5 (2009) 103.
- [113] C. Kleinstreuer, Y. Feng, *Nanoscale Res. Lett.* 6 (2011) 229.
- [114] X. Zhang, H. Gu, M. Fujii, *Exp. Therm. Fluid Sci.* 31 (2007) 593.
- [115] J.-H. Lee, K.S. Hwang, S.P. Jang, B.H. Lee, J.H. Kim, S.U.S. Choi, C.J. Choi, *Int. J. Heat Mass Tran.* 51 (2008) 2651.
- [116] M. Chopkar, S. Sudarshan, P.K. Das, I. Manna, *Metall Mater Trans. A* 39 (2008) 1535.

- [117] D. Zhu, X. Li, N. Wang, X. Wang, J. Gao, H. Li, *Curr. Appl. Phys.* 9 (2009) 131.
- [118] L. Chen, H. Xie, *Colloid Surface A: Physicochem. Eng. Aspects* 352 (2009) 136.
- [119] W. Duangthongsuk, S. Wongwises, *Exp. Therm. Fluid Sci.* 33 (2009) 706.
- [120] M. Chandrasekar, S. Suresh, A. Chandra Bose, *Exp. Therm. Fluid Sci.* 34 (2010) 210.
- [121] T.-P. Teng, Y.-H. Hung, T.-C. Teng, H.-E. Mo, H.-G. Hsu, *Appl. Therm. Eng.* 30 (2010) 2213.
- [122] M. Kole, T.K. Dey, *Exp. Therm. Fluid Sci.* 35 (2011) 1490.
- [123] S.W. Lee, S.D. Park, S. Kang, I.C. Bang, J.H. Kim, *Int. J. Heat Mass Tran.* 54 (2011) 433.
- [124] M. Hojjat, S.G. Etamad, R. Bagheri, J. Thibault, *Int. J. Heat Mass Tran.* 54 (2011) 1017.
- [125] W. Yu, H. Xie, Y. Li, L. Chen, *Particuology* 9 (2011) 187.
- [126] R. Karthik, R. Harish Nagarajan, B. Raja, P. Damodharan, *Exp. Therm. Fluid Sci.* 40 (2012) 1.
- [127] A. Gavili, F. Zabihi, T.D. Isfahani, J. Sabbaghzadeh, *Exp. Therm. Fluid Sci.* 41 (2012) 94.
- [128] T. Yiamsawasd, A.S. Dalkilic, S. Wongwises, *Thermochim. Acta* 545 (2012) 48.
- [129] M. Wan, R.R. Yadav, K.L. Yadav, S.B. Yadav, *Exp. Therm. Fluid Sci.* 41 (2012) 158.
- [130] A. Nasiri, M. Shariaty-Niasar, A.M. Rashidi, R. Khodafarin, *Int. J. Heat Mass Tran.* 55 (2012) 1529.
- [131] C. Pang, J.-Y. Jung, J.W. Lee, Y.T. Kang, *Int. J. Heat Mass Tran.* 55 (2012) 5597.
- [132] S.M.S. Murshed, K.C. Leong, C. Yang, *Int. J. Therm. Sci.* 47 (2008) 560.
- [133] S. Özerinç, S. Kakaç, A. Yazıcıoğlu, *Microfluid Nanofluid* 8 (2010) 145.
- [134] K.S. Hong, T.-K. Hong, H.-S. Yang, *Appl. Phys. Lett.* 88 (2006) 031901.
- [135] J.J. De Groot, J. Kestin, H. Sookiazian, *Physica* 75 (1974) 454.
- [136] A. Santucci, L. Verdini, P.G. Verdini, *Rev. Sci. Instrum.* 57 (1986) 1627.
- [137] B.L. Neindre, R. Tufeu, A.M. Sirota, *Experimental Thermodynamics, Vol. III: Measurement of the Transport Properties of Fluids*, Blackwell Scientific, Oxford, 1991.
- [138] J.A. Eastman, S.R. Phillpot, S.U.S. Choi, P. Keblinski, *Ann. Rev. Mater. Res.* 34 (2004) 219.
- [139] Y. Nagasaka, A. Nagashima, *J. Phys. E: Scientific Instruments* 14 (1981) 1435.
- [140] G. Paul, M. Chopkar, I. Manna, P.K. Das, *Renew. Sust. Energ. Rev.* 14 (2010) 1913.
- [141] P. Bhattacharya, S. Nara, P. Vijayan, T. Tang, W. Lai, P.E. Phelan, R.S. Prasher, D.W. Song, J. Wang, *Int. J. Heat and Mass Tran.* 49 (2006) 2950.
- [142] D.J. Jeffrey, *Proc. R. Soc. Lond. Ser. A* 335 (1973) 355.
- [143] R.H. Davis, *Int. J. Thermophys.* 7 (1986) 609.
- [144] R.L. Hamilton, O.K. Crosser, *IEC Fundam.* 1 (1962).
- [145] B.X. Wang, L.P. Zhou, X.F. Peng, *Int. J. Heat Mass Tran.* 46 (2003) 2665.
- [146] W. Yu, S.U.S. Choi, *J. Nanopart. Res.* 5 (2003) 167.
- [147] Y. Xuan, Q. Li, W. Hu, *AIChE Journal* 49 (2003) 1038.
- [148] P. Bhattacharya, S.K. Saha, A. Yadav, P.E. Phelan, R.S. Prasher, *J. Appl. Phys.* 95 (2004) 6492.
- [149] S.P. Jang, S.U.S. Choi, *Appl. Phys. Lett.* 84 (2004) 4316.
- [150] J. Koo, C. Kleinstreuer, *J. Nanopart. Res.* 6 (2004) 577.
- [151] Q. Xue, W.-M. Xu, *Mater. Chem. Phys.* 90 (2005) 298.
- [152] K.C. Leong, C. Yang, S.M.S. Murshed, *J. Nanopart. Res.* 8 (2006) 245.
- [153] C. Sitprasert, P. Dechaumphai, V. Juntasaro, *J. Nanopart. Res.* 11 (2009) 1465.
- [154] L. Yang, K. Du, *Int. J. Refrig.* 35 (2012) 1978.
- [155] P. Keblinski, S.R. Phillpot, S.U.S. Choi, J.A. Eastman, *Int. J. Heat Mass Tran.* 45 (2002) 855.
- [156] G.H. Kumar, H.E. Patel, V.R.R. Kumar, T. Sundararajan, T. Pradeep, S.K. Das, *Phys. Rev. Lett.* 93 (2004) 144301.
- [157] R. Prasher, *Phys. Rev. Lett.* 94 (2005) 025901.
- [158] Y. Ren, H. Xie, A. Cai, *J. Phys. D: Appl. Phys.* 39 (2005) 3958.
- [159] L. Gao, X.F. Zhou, *Phys. Lett. A* 348 (2006) 355.
- [160] J.A. Eastman, S.R. Phillpot, S.U.S. Choi, P. Keblinski, *Annu. Rev. Mater. Res.* 34 (2004) 219.
- [161] M. Kole, T.K. Dey, *Thermochim. Acta* 535 (2012) 58.
- [162] P. Keblinski, S.R. Phillpot, S.U.S. Choi, J.A. Eastman, *Int. J. Heat Mass Tran.* 45 (2002) 855.
- [163] A. Boushehri, E. Kafshdare Goharshad, *High Temp.-*

- High Press. (1993).
- [164] L. Wang, J. Fan, *Nanoscale Res. Lett.* 6 (2011) 1.
- [165] M. Kole, T.K. Dey, *Exp. Therm. Fluid Sci.* 34 (2010) 677.
- [166] I.M. Mahbubul, R. Saidur, M.A. Amalina, *Int. J. Heat Mass Tran.* 55 (2012) 874.
- [167] Z. Meng, D. Han, D. Wu, H. Zhu, Q. Li, *Procedia Eng* 36 (2012) 521.
- [168] P.K. Namburu, D.P. Kulkarni, D. Misra, D.K. Das, *Exp. Therm. Fluid Sci.* 32 (2007) 397.
- [169] H. Chen, Y. Ding, Y. He, C. Tan, *Chem. Phys. Lett.* 444 (2007) 333.
- [170] E.N. Andrad, *Philos. Mag.* 17 (1934) 497.
- [171] H. Vogel, *Physick Z* 22 (1921) 645.
- [172] G.S. Fulcher, *J. Am. Ceram. Soc.* 8 (1925) 339.
- [173] E.K. Goharshadi, M. Hadadian, *Ceram. Int.* 38 (2012) 1771.
- [174] M.J. Pastoriza-Gallego, C. Casanova, J.L. Legido, M.M. Piñeiro, *Fluid Phase Equilib.* 300 (2011) 188.
- [175] M. Abareshi, S.H. Sajjadi, S.M. Zebarjad, E.K. Goharshadi, *J. Mol. Liq.* 163 (2011) 27.
- [176] Q. Li, Y. Xuan, J. Wang, *Exp. Therm. Fluid Sci.* 30 (2005) 109.
- [177] L. Fedele, L. Colla, S. Bobbo, *Int. J. Refrigeration* 35 (2012) 1359.
- [178] M. Hojjat, S.G. Etemad, R. Bagheri, J. Thibault, *International Commun. Heat Mass Tran.* 38 (2011) 144.
- [179] R.B. Mansour, N. Galanis, C.T. Nguyen, *Appl. Therm. Eng.* 27 (2007) 240.
- [180] B.H.C. J. *Chem. Phys.* 20 (1952) 5.
- [181] N.A. Frankel, A. Acrivos, *Chem. Eng. Sci.* 22 (1967) 847.
- [182] T.S. Lundgren, *J. Fluid Mech.* 51 (1972) 273.
- [183] G.K. Batchelor, *J. Fluid Mech.* 83 (1977) 97.
- [184] A. Graham, *Appl. Sci. Res.* 37 (1981) 275.
- [185] W.J. Tseng, C.-N. Chen, *Mat. Sci. Eng.: A* 347 (2003) 145.
- [186] N.-S. Cheng, A.W.-K. Law, *Powder Technol.* 129 (2003) 156.
- [187] K. Toda, H. Furuse, *J. Biosci. Bioeng.* 102 (2006) 524.
- [188] C.T. Nguyen, F. Desgranges, G. Roy, N. Galanis, T. Maré, S. Boucher, H. Angue Mintsu, *Int. J. Heat Fluid Flow* 28 (2007) 1492.
- [189] N.S.N. Masoumi, A. Behzadmeh, *J. Phys. D: Appl. Phys.* 42 (2009).
- [190] L. Yang, K. Du, Y.H. Ding, B. Cheng, Y.J. Li, *Powder Technol.* 215-216 (2012) 210.
- [191] S.E.B. Maïga, S.J. Palm, C.T. Nguyen, G. Roy, N. Galanis, *Int. J. Heat Fluid Flow* 26 (2005) 530.
- [192] W. Duangthongsuk, S. Wongwises, *Int. Commun. Heat Mass Tran.* 35 (2008) 1320.
- [193] B.C. Pak, Y.I. Cho, *Exp. Heat Tran.* 11 (1998) 151.
- [194] Y. Xuan, W. Roetzel, *Int. J. Heat Mass Tran.* 43 (2000) 3701.
- [195] R.-H. Chen, T. X. Phuoc, D. Martello, *Int. J. Heat Mass Tran.* 54 (2011) 2459.
- [196] S. Tanvir, L. Qiao, *Nano. Res. Lett.* 7 (2012) 226.
- [197] M.J. Assael, I.N. Metaxa, K. Kakosimos, D. Constantinou, *Int. J. Thermophys.* 27 (2006) 999.
- [198] D.G. Cahill, W.K. Ford, K.E. Goodson, G.D. Mahan, A. Majumdar, H.J. Maris, R. Merlin, S.R. Phillpot, *J. Appl. Phys.* 93 (2003) 793.
- [199] D.A. McQuarrie, *Statistical Mechanics*, Harper & Row, New York, 1976.
- [200] W.G. Hoover, *Computational Statistical Mechanics*, Elsevier, Amsterdam, 1991.
- [201] L. Xue, P. Keblinski, S.R. Phillpot, S.U.S. Choi, J.A. Eastman, *Int. J. Heat Mass Tran.* 47 (2004) 4277.
- [202] S. Shenogin, L. Xue, R. Ozisik, P. Keblinski, D.G. Cahill, *J. Appl. Phys.* 95 (2004) 8136.
- [203] Y. Xuan, K. Yu, Q. Li, *Prog. Comput. Fluid Dynamics* 5 (2005) 13.
- [204] M. Vladkov, J.L. Barrat, *Nano Lett.* 6 (2006) 1224.
- [205] R. Prasher, W. Evans, P. Meakin, J. Fish, P. Phelan, P. Keblinski, *Appl. Phys. Lett.* 89 (2006) 143119.
- [206] J. Eapen, J. Li, S. Yip, *Phys. Rev. Lett.* 98 (2007) 028302.
- [207] J. Eapen, J. Li, S. Yip, *Phys. Rev. E* 76 (2007) 062501.
- [208] S. Sarkar, R.P. Selvam, *J. Appl. Phys.* 102 (2007) 074302.
- [209] L. Li, Y. Zhang, H. Ma, M. Yang, *Phys. Lett. A* 372 (2008) 4541.
- [210] M.B. Vladkov, Jean-Louis, *J. Comput. Theoretical Nanosci.* 5 (2008) 7.
- [211] N. Sankar, N. Mathew, C.B. Sobhan, *Int. Commun. Heat Mass Tran.* 35 (2008) 867.

- [212] W.Q. Lu, Q.M. Fan, Eng. Anal. Bound. Elem 32 (2008) 282.
- [213] A. Mohebbi, J. Mol. Liq. 175 (2012) 51.
- [214] H. Kang, Y. Zhang, M. Yang, L. Li, Phys. Lett. A 376 (2012) 521.
- [215] H.R. Seyf, M. Feizbakhshi, Int. J. Therm. Sci. 58 (2012) 168.
- [216] L.X. Dang, H.V.R. Annapureddy, X. Sun, P.K. Thallapally, B. Peter McGrail, Chem. Phys. Lett. 551 (2012) 115.
- [217] Y.S. Lin, P.Y. Hsiao, C.C. Chieng, Int. J. Therm. Sci. 62 (2012) 56.
- [218] W. Gao, L. Kong, P. Hodgson, Int. J. Heat Mass Tran. 55 (2012) 5007.
- [219] C.Y. Tsai, H.T. Chien, P.P. Ding, B. Chan, T.Y. Luh, P.H. Chen, Mater. Lett. 58 (2004) 1461.
- [220] S.C. Tzeng, C.W. Lin, K.D. Huang, Acta Mech. 179 (2005) 11.
- [221] C.T. Nguyen, G. Roy, C. Gauthier, N. Galanis, Appl. Therm. Eng. 27 (2007) 1501.
- [222] K.-J. Park, D. Jung, Energ. Buildings 39 (2007) 1061.
- [223] C. Choi, H.S. Yoo, J.M. Oh, Curr. Appl. Phys. 8 (2008) 710.
- [224] K.Y. Leong, R. Saidur, S.N. Kazi, A.H. Mamun, Appl. Therm. Eng. 30 (2010) 2685.
- [225] P.E. Phelan, R.S. Prasher, G. Rosengarten, R.A. Taylor, J. Renew. Sust. Energ. 2 (2010) 033102.
- [226] E. Firouzfard, M. Soltanieh, S.H. Noie, S.H. Saidi, Appl. Therm. Eng. 31 (2011) 1543.
- [227] V. Vasu, K.M. Kumar, Nano-Micro Lett. 3 (2011) 209.
- [228] T. Yousefi, F. Veysi, E. Shojaeizadeh, S. Zinadini, Renew. Energ. 39 (2012) 293.
- [229] R. Saidur, T.C. Meng, Z. Said, M. Hasanuzzaman, A. Kamyar, Int. J. Heat Mass Tran. 55 (2012) 5899.
- [230] A. Ijam, R. Saidur, Appl. Therm. Eng. 32 (2012) 76.
- [231] M. Keshavarz Moraveji, S. Razvarz, Int. Commun. Heat Mass Tran. 39 (2012) 1444.
- [232] T.H. Wu, T. Teslaa, SherazKalim, Christopher T. French, ShahriarMoghadam, Randolph Wall, Jeffery F. Miller, Owen N. Witte, Michael A. Teitell, P.-Y. Chiou, Anal. Chem. 83 (4) (2011) 7.
- [233] W.Y.a.H. Xie, J. Nanomater. 2012 (2012).
- [234] C. Zhang, M. Wang, H. Han, X. Cao, BioTechniques 44 (2008) 9.
- [235] P. Keblinski, J.A. Eastman, D.G. Cahill, Mater. Today 8 (2005) 36.